Journal of Experimental Botany, Vol. 59, No. 7, pp. 1715–1734, 2008
doi:10.1093/jxb/ern028 Advance Access publication 26 March, 2008

Journal of Experimental Botany
www.jxb.oxfordjournals.org

SPECIAL ISSUE RESEARCH PAPER

Structural, biochemical, and physiological characterization of photosynthesis in two C_4 subspecies of *Tecticornia indica* and the C_3 species *Tecticornia pergranulata* (Chenopodiaceae)

Elena V. Voznesenskaya[1], Hossein Akhani[2], Nuria K. Koteyeva[1], Simon D. X. Chuong[3], Eric H. Roalson[4], Olavi Kiirats[4], Vincent R. Franceschi[4] and Gerald E. Edwards[4,*]

[1] *Laboratory of Anatomy and Morphology, V. L. Komarov Botanical Institute of Russian Academy of Sciences, Prof. Popov Street 2, 197376, St Petersburg, Russia*

[2] *Department of Plant Sciences, School of Biology, College of Sciences, University of Tehran, PO Box 14155-6455, Tehran, Iran*

[3] *Department of Biology, University of Waterloo, Waterloo, Ontario N2L 3G1, Canada*

[4] *School of Biological Sciences, Washington State University, Pullman, WA 99164-4236, USA*

Received 4 September 2007; Revised 16 January 2008; Accepted 21 January 2008

Abstract

Among dicotyledon families, Chenopodiaceae has the most C_4 species and the greatest diversity in structural forms of C_4. In subfamily Salicornioideae, C_4 photosynthesis has, so far, only been found in the genus *Halosarcia* which is now included in the broadly circumscribed *Tecticornia*. Comparative anatomical, cytochemical, and physiological studies on these taxa, which have near-aphyllous photosynthetic shoots, show that *T. pergranulata* is C_3, and that two subspecies of *T. indica* (*bidens* and *indica*) are C_4 (Kranz-tecticornoid type). In *T. pergranulata*, the stems have two layers of chlorenchyma cells surrounding the centrally located water storage tissue. The two subspecies of *T. indica* have Kranz anatomy in reduced leaves and in the fleshy stem cortex. They are NAD-malic enzyme-type C_4 species, with mesophyll chloroplasts having reduced grana, characteristic of this subtype. The Kranz-tecticornoid-type anatomy is unique among C_4 types in the family in having groups of chlorenchymatous cells separated by a network of large colourless cells (which may provide mechanical support or optimize the distribution of radiation in the tissue), and in having peripheral vascular bundles with the phloem side facing the bundle sheath cells. Also, the bundle sheath cells have chloroplasts in a centrifugal position, which is atypical for C_4 dicots. Fluorescence analyses in fresh sections indicate that all non-lignified cell walls have ferulic acid, a cell wall cross-linker. Structural–functional relationships of C_4 photosynthesis in *T. indica* are discussed. Recent molecular studies show that the C_4 taxa in *Tecticornia* form a monophyletic group, with incorporation of the Australian endemic genera of Salicornioideae, including *Halosarcia*, *Pachycornia*, *Sclerostegia*, and *Tegicornia*, into *Tecticornia*.

Key words: C_3 plants, C_4 plants, Chenopodiaceae, chloroplast ultrastructure, *Halosarcia*, immunolocalization, NAD-ME type, photosynthetic enzymes, phylogeny, *Tecticornia*.

Introduction

In the family Chenopodiaceae, which has C_3 and C_4 species, all C_4 genera occur in subfamily Chenopodioideae (*Atriplex*) and in a succulent clade made up of three

* To whom correspondence should be addressed. E-mail: edwardsg@wsu.edu

Abbreviations: BS, bundle sheath; BSC, bundle sheath cell; C_i, intercellular levels of CO_2; CW, cell wall; Γ^*, CO_2 compensation point based on Rubisco carboxylase/oxygenase activity; GDC, glycine decarboxylase; MC, mesophyll cell; ML, maximum likelihood; NAD-ME, NAD-malic enzyme; NADP-ME, NADP-malic enzyme; PEPC, phophoenolpyruvate carboxylase; PEP-CK, phosphoenolpyruvate carboxykinase; PPDK, pyruvate; Pi, dikinase; PPFD, photosynthetic photon flux density; WS, water storage.

subfamilies: Suaedoideae (*Suaeda* and *Bienertia*), Salsoloideae (various genera), and Salicornioideae (*Halosarcia*) (Carolin *et al*., 1975; Pyankov, 1991; Akhani *et al*., 1997; Jacobs, 2001; Pyankov *et al*., 2001*a*; Kadereit *et al*., 2003; Kapralov *et al*., 2006; Akhani and Ghasemkhani, 2007). This family has the largest number of C_4 species and also the greatest diversity in leaf anatomy among dicot families, including C_4 Kranz and C_4 single-cell type species, as well as C_3 type species (Carolin *et al*., 1975; Sage *et al*., 1999; Edwards *et al*., 2004). Six C_4 types of Kranz anatomy (atriplicoid, kochioid, salsoloid, halosarcoid, and, in the genus *Suaeda*, salsina and schoberia types) and five C_3 types (axyroid, corispermoid, austrobassioid, neokochioid, and sympegmoid) have been described among species of this family, mostly in corresponding genera (Carolin *et al*., 1975, 1982; Voznesenskaya, 1976*b*; Voznesenskaya and Gamaley, 1986; Jacobs, 2001; Kadereit *et al*., 2003). Recently, leaf anatomy in representative Chenopodiaceae species was further revised with the description of 15 C_4 types (Kadereit *et al*., 2003). The C_4 types of anatomy vary in the structure and arrangement of the two-layered chlorenchyma adjacent to the vascular bundles, and by the presence or absence of water storage (WS) tissue, hypodermal cells, and sclerenchyma, and whether they have continuous or interrupted Kranz tissue.

Species in subfamily Salicornioideae are hygrohalophytic plants which belong to the most salt-tolerant angiosperms inhabiting salt marshes and inland saline habitats. In this subfamily, only one species, *Halosarcia indica*, has been identified as C_4 on the basis of its anatomy and C_4-type carbon isotope composition, while 11 species of this genus have C_3-type carbon isotope composition (Wilson, 1980; Carolin *et al*., 1982; Akhani *et al*., 1997).

Carolin *et al*. (1982) studied the anatomical structure in several representatives of the genus *Halosarcia*. Species with C_3-type carbon isotope values had 2–3 layers of chlorenchyma tissue surrounding WS parenchyma, while several subspecies of *H. indica* had C_4-type isotope values and Kranz anatomy. Unlike the salsoloid type of Kranz anatomy, an unusual occurrence of colourless (or, more accurately, organelle-deficient) cells between groups of chlorophyllous mesophyll cells (MCs) was reported in *H. indica*.

Halosarcia was segregated from *Arthrocnemum* by Wilson (1980) by the absence of sclereids in chlorenchyma tissue and by the flowers having a single stamen. According to recent phylogenies, *Halosarcia* is placed in a monophyletic clade with four other Australian endemic genera, including *Tecticornia*, *Pachycornia*, *Sclerostegia*, and *Tegicornia* (Shepherd *et al*., 2004; Kadereit *et al*., 2006). Shepherd and Wilson (2007) have incorporated all these genera into a broadly defined *Tecticornia* s. l. which is accepted in this paper.

The aim of the present study was to characterize the anatomy and ultrastructure of chlorenchyma, and the unusual occurrence of colourless cells within Kranz anatomy, to identify the C_4 biochemical subtype, and analyse features of CO_2 fixation in *T. indica* (using two subspecies which occur on different continents and are visibly different, *bidens* and *indica*). Comparative analyses were made with the C_3 species *T. pergranulata*. The phylogenetic position of these representatives of *Tecticornia* in subfamily Salicornioideae was also evaluated.

Materials and methods

Plant material

Seeds of *T. pergranulata* (J. M. Black) K. A. Sheph. & Paul G. Wilson subsp. *pergranulata* and *T. indica* subsp. *bidens* (Nees) K. A. Sheph. & Paul G. Wilson were provided by G Barrett, Greg Barrett & Associates, Darlington, Western Australia. Seeds of *T. indica* (Willd.) K. A. Sheph. & Paul G. Wilson subsp. *indica* were collected by H Akhani from Pakistan, 40 km NW of Karachi (H. Akhani 16537). Seeds were stored at 3–5 °C prior to use, then germinated on moist paper in Petri dishes in a growth chamber at 30/25 °C and a photosynthetic photon flux density (PPFD) of 75 μmol m^{-2} s^{-1} with a 14/10 h light/dark photoperiod. The seedlings were then transplanted to 10 cm diameter pots with commercial potting soil and grown for 3 d under the same regime. Established plants were then transferred to a growth chamber (model GC-16; Enconair Ecological Chambers Inc., Winnipeg, Canada) and grown under ~400 PPFD with a 16/8 h light/dark photoperiod and 25/18 °C day/night temperature regime. For microscopy and biochemical analyses, samples of mature segments were taken from ~2.5- to 3-month-old plants.

Voucher specimens are available at the Marion Ownbey Herbarium, Washington State University: *T. pergranulata* (E. Voznesenskaya 28), April 2006, WS 369799; *T. indica* subsp. *indica* (E. Voznesenskaya 29), April 2006, WS 369801; *T. indica* subsp. *bidens* (E. Voznesenskaya 27), April 2006, WS 369800.

Light and electron microscopy

Hand-cut sections of fresh stems were placed in water and studied under a light stereo microscope. The area of chlorenchyma tissue external to the central cylinder, and of WS tissue, as a percentage of the total cross-sectional area was determined from digital images (on ~10 cross-sections taken from two different plants) using UTHSCSA, Image Tool for Windows, version 3.00, University of Texas Health Science Center, San Antonio, TX, USA.

For microscopy on fixed material, samples were taken from 2–3 plants (5–6 samples from 2–3 branches of each plant). Samples for structural studies were fixed at 4 °C in 2% (v/v) paraformaldehyde and 2% (v/v) glutaraldehyde in 0.1 M phosphate buffer (pH 7.2), post-fixed in 2% (w/v) OsO_4, and then, after a standard acetone dehydration procedure, embedded in Spurr's epoxy resin. Cross-sections were made on a Reichert Ultracut R ultramicrotome (Reichert-Jung GmbH, Heidelberg, Germany). For light microscopy, semi-thin sections were stained with 1% (w/v) toluidine blue O in 1% (w/v) $Na_2B_4O_7$. Ultra-thin sections were stained for transmission electron microscopy with 2% (w/v) uranyl acetate followed by 2% (w/v) lead citrate. Hitachi H-600 (Hitachi Scientific Instruments, Mountain View, CA, USA) and JEOL JEM-1200 EX (JEOL USA, Inc., Peabody, MA, USA) transmission electron microscopes were used for observation and photography.

For scanning electron microscopy (SEM), leaf samples were fixed at 4 °C in 2% (v/v) paraformaldehyde and 2% (v/v) glutaraldehyde in 0.1 M phosphate buffer (pH 7.2), post-fixed in 2% (w/v) OsO_4, and then dehydrated in an ethanol series to 100% ethanol, cryofractured in liquid nitrogen, critical-point dried, attached to SEM mounts, sputter-coated with gold, and observed with a Hitachi S570 SEM (Hitachi, Ltd, Tokyo, Japan).

The size of chloroplasts and mitochondria, and the thickness of cell walls (CWs), were measured on micrographs from leaf cross-sections with an image analysis program (Image Tool for Windows). For measurements of the length and width, images of chloroplast median sections were used. For determining the size of mitochondria, the small diameter of profiles on cross-sections was measured. As was previously noted in quantitative studies on mitochondria, rather long profiles can occasionally be observed in microscopy sections; however, only the small diameter will reflect the difference in size between different tissues or species (see Voznesenskaya *et al*., 2007).

Fluorescence of chloroplasts and cell walls, and lignification

Hand-cut sections of leaves or stems were placed on slides in distilled water and examined under UV light [with a 4′,6-diamidino-2-phenylindole (DAPI) filter] with a Zeiss LSM 510 META (Jena, Germany) microscope. For comparison, similar sections were treated with 0.1 M NH_4OH to reveal the presence of CW-bound ferulic acid. According to Harris and Hartley (1976, 1980), Hartley and Harris (1981), and Rudall and Caddick (1994), if the tissue contains CW-bound ferulic acid, an increase of the pH (to ~10.3) will change the blue fluorescence of CWs to blue-green by ionization of the phenol OH group. This treatment does not change the autofluorescence of CWs in lignified or suberized tissues. To detect the position of lignified tissue, sections were treated for 1 h with phloroglucinol (2% in 10% HCl), which stains lignin-containing CWs red, while for detection of suberization, sections were stained with Sudan IV in 70% alcohol, which stains suberized CWs dark red (Ruzin, 1999).

In situ *immunolocalization*

Leaf samples were fixed at 4 °C in 2% (v/v) paraformaldehyde and 1.25% (v/v) glutaraldehyde in 0.05 M PIPES buffer, pH 7.2. The samples were dehydrated with a graded ethanol series and embedded in London Resin White (LR White, Electron Microscopy Sciences, Fort Washington, PA, USA) acrylic resin. Antibodies used (all raised in rabbit) were anti-*Spinacia oleracea* L. Rubisco (LSU) IgG (courtesy of B McFadden), commercially available anti-*Zea mays* L. phosphoenolpyruvate carboxylase (PEPC) IgG (Chemicon, Temecula, CA, USA), anti-pyruvate, Pi dikinase (PPDK) IgG (courtesy of T Sugiyama), anti-*Amaranthus hypochondriacus* L. mitochondrial NAD-malic enzyme (NAD-ME) IgG (courtesy of J Berry), which was prepared against the 65 kDa α-subunit (Long and Berry, 1996), and anti-*Pisum sativum* L. glycine decarboxylase (GDC) against the P subunit (courtesy of D Oliver). Pre-immune serum was used in all cases for controls.

Cross-sections, 0.8–1 μm thick, were dried from a drop of water onto gelatin-coated slides and blocked for 1 h with TBST+BSA [10 mM TRIS-HCl, 150 mM NaCl, 0.3% (v/v) Tween-20, 1% (w/v) bovine serum albumin, pH 7.2]. They were then incubated for 3 h with either pre-immune serum diluted in TBST+BSA (1:100), anti-Rubisco LSU (1:500), or anti-PEPC (1:200). The slides were washed with TBST+BSA and then treated for 1 h with protein A–gold (10 nm particles diluted 1:100 with TBST+BSA). After washing, the sections were exposed to a silver enhancement reagent for 20 min according to the manufacturer's directions (Amersham, Arlington Heights, IL, USA), stained with 0.5% (w/v) Safranin O, and imaged in a reflected/transmitted mode using a BioRad 1024 confocal system with a Nikon Eclipse TE 300 inverted microscope and Lasergraph image program 3.10. The background labelling with pre-immune serum was very low, although some infrequent labelling occurred in areas where the sections were wrinkled due to trapping of antibodies/label (results not shown).

For TEM immunolabelling, thin sections on Formvar-coated nickel grids were incubated for 1 h in TBST+BSA to block non-specific protein binding on the sections. They were then incubated for 3 h with either the pre-immune serum diluted in TBST+BSA (1:50) or anti-PEPC (1:20), anti-Rubisco (1:50), anti-PPDK (1:40), anti-NAD-ME (1:50), or anti-GDC (1:50) antibodies. After washing with TBST+BSA, the sections were incubated for 1 h with protein A–gold (10 or 15 nm) diluted 1:100 with TBST+BSA. The sections were washed sequentially with TBST+BSA, TBST, and distilled water, and then post-stained with a 1:4 dilution of 1% (w/v) potassium permanganate and 2% (w/v) uranyl acetate. Images were collected using a JEOL JEM-1200 EX transmission electron microscope. The density of labelling was determined by counting the gold particles on electron micrographs and calculating the number per unit area (μm^2).

Staining for polysaccharides

The periodic acid–Schiff's procedure (PAS) was used for staining starch in sectioned materials. Sections, 0.8–1 μm thick, were made from the same samples used for immunolocalization, dried onto gelatin-coated slides, incubated in periodic acid [1% (w/v)] for 30 min, washed, and then incubated with Schiff's reagent (Sigma, St Louis, MO, USA) for 1 h. After rinsing, the sections were ready for analysis by light microscopy. CWs and starch stained bright reddish pink, while other elements of the cells (cytoplasm) remained unstained. Controls lacking the periodic acid treatment (required for oxidation of the polysaccharides giving rise to Schiff's-reactive groups) showed little or no background staining (not shown).

Western blot analysis

Total proteins were extracted from leaves by homogenizing 500 mg of tissue in 1 ml of extraction buffer [100 mM TRIS-HCl, pH 7.5, 5 mM $MgSO_4$, 10 mM dithiothreitol, 5 mM EDTA, 0.5% (w/v) SDS, 2 % (v/v) β-mercaptoethanol, 10% (v/v) glycerol, 1 mM phenylmethylsulphonyl fluoride, and 25 μg ml^{-1} each of aprotinin, leupeptin, and pepstatin]. After centrifugation at high speed for 3 min in a microcentrifuge, the supernatant was collected and the protein concentration was determined by Bradford protein assay (Bio-Rad) using BSA as a standard. Protein samples (10 μg) were separated by 12.5% SDS–PAGE, blotted onto nitrocellulose, and probed with anti-*A. hypochondriacus* NAD-ME (1:5000), anti-*Z. mays* NADP-malic enzyme (NADP-ME), courtesy of C Andreo (Maurino *et al*., 1996) (1:5000), anti-*Z. mays* PEPC (1:10 000), anti-*Z. mays* PPDK (1:5000), anti-*Urochloa maxima* phosphoenolpyruvate carboxykinase (PEP-CK), courtesy of RC Leegood, or anti-*Spinacia oleracea* Rubisco LSU (1:10 000) overnight at 4 °C. Goat anti-rabbit IgG–alkaline phosphatase conjugate antibody (Bio-Rad) was used at a dilution of 1:50 000 for detection. Bound antibodies were localized by developing the blots with 20 mM nitroblue tetrazolium and 75 mM 5-bromo-4-chloro-3-indolyl phosphate in the detection buffer (100 mM TRIS-HCl, pH 9.5, 100 mM NaCl, and 5 mM $MgCl_2$).

Acidity

Plant samples were collected just before the beginning of the light period, in the middle of the day, and in the late afternoon just before the beginning of the dark period. Samples of known fresh weight (between 0.2 g and 0.5 g) were ground in 2 ml of distilled water.

The sample was titrated with 0.01 M NaOH to a pH 7 end point using a pH meter, and the μeq acid per g fresh weight was calculated.

Measurements of rates of photosynthesis

Rates of photosynthesis in response to light were measured with a CO_2 analyser (ADC LCPro+, ADC BioScientific Ltd, Hoddesdon, UK) operating in a differential mode. The air temperature was 25±0.5 °C (stem temperature was 25–27 °C), the minimum humidity was 12.0±0.5 mbar, and the flow rate was 200 μmol s^{-1}. The local average barometric pressure, as determined by the CO_2 analysing system, was 922.3±3.4 mbar.

For each experiment, part of a branch of an intact plant (3–4 months old) was enclosed in the conifer chamber designed for terete or semi-terete leaves. The branch was illuminated with 920 PPFD under 370 μbar CO_2 until a steady-state rate of CO_2 fixation was obtained (generally 40–50 min). For varying light experiments at 370 μbar CO_2, measurements were made beginning at 1380 PPFD, followed by decreasing increments of light intensity at 4 min intervals.

For measurement of the response of photosynthesis to varying CO_2 at 2% and 21% O_2, and for determining the CO_2 compensation point based on Rubisco carboxylase/oxygenase activity (Γ^*), gas exchange was measured with the FastEst gas system (see Laisk and Edwards, 1997; Sun *et al*., 1999). A branch was enclosed in a small leaf chamber (4 cm×3 cm×0.5 cm) with an open gas flow rate of 0.5 mmol s^{-1}. The chamber temperature was maintained at 25 °C, with the water jacket of the chamber connected to a thermostated water bath. Both sides of the branch were illuminated with a PPFD of 900 μmol quanta m^{-2} s^{-1} (measured with a Li-Cor 185 quantum sensor) at the glass window by fibreoptics with a Schott KL1500 source (H Walz, Effeltrich, Germany). Relative humidity in the leaf chamber was controlled by diverting part of the air flow stream through air that was equilibrated with water at 50 °C. CO_2 and O_2 partial pressures were obtained by mixing pure CO_2, O_2, N_2, and CO_2-free air with the help of capillaries. The pressure difference in the capillaries was stabilized by manostats (tubes with open ends submerged in water to adjustable heights). The water vapour pressure was measured with a psychrometer. CO_2 exchange was measured with a MK3-225 IR gas analyser (ADC, Hoddesdon, Hertfordshire, UK) or a Li-6251 analyser (Li-Cor, Lincoln, NE, USA). Data were recorded by computer using an A/D board ME-30 and a RECO program, and analysed by computer programs ANAL and SYNTE. The programs RECO and ANAL were written by V Ova (University of Tartu, Estonia) in Turbo-Pascal. The intercellular CO_2 concentration in the leaf was calculated with inputs for the rate of photosynthesis, the CO_2 concentration in the air, and the diffusive resistance of CO_2 from the atmosphere to the intercellular space. The latter was calculated by determining the diffusive resistance to water by measuring transpiration, and the water vapour concentration difference from the leaf to air (for a description see Ku *et al*., 1977; von Caemmerer and Farquhar, 1981). The Γ^*, where the rate of CO_2 uptake equals photorespiratory loss of CO_2, was determined by taking the co-ordinates of the intersection of CO_2 response curves measured at different light intensities (Brooks and Farquhar, 1985).

The area of tissue exposed to incident light was calculated by taking a digital image of the branch that was enclosed in the chamber, and then determining the exposed branch area using an image analysis program (Image Tool for Windows).

$\delta^{13}C$ values

Measures of the carbon isotope composition ($\delta^{13}C$ values) were made at Washington State University on leaf and stem samples taken from plants using a standard procedure relative to PDB (Pee Dee Belemnite) limestone as the carbon isotope standard (Bender *et al*., 1973). Plant samples (from plants growing in the Washington State University School of Biological Sciences growth chamber) were dried at 80 °C for 24 h, milled to a fine powder, and then 1–2 mg were placed in a tin capsule and combusted in a Eurovector elemental analyser. The resulting N_2 and CO_2 gases were separated by gas chromatography and admitted into the inlet of a Micromass Isoprime isotope ratio mass spectrometer (IRMS) for determination of $^{13}C/^{12}C$ ratios (R). $\delta^{13}C$ values were determined where $\delta=1000\times(R_{sample}/R_{standard})-1$.

Statistics

Where indicated, standard errors were determined, and analysis of variance (ANOVA) was performed with Statistica 7.0 software (StatSoft, Inc.). Tukey's HSD (honest significant difference) tests were used to analyse differences between cell types. All analyses were performed at the 95% significance level.

Results

General features including the stem surface

Plants of all three representatives are prostrate to erect shrubs and subshrubs with stems comprised of segments with intercalary growth. These plants have reduced opposite leaves (~1 mm in length) at the distal (top) end of each segment (Fig. 1B, G, L). Photosynthesis is accomplished in the fleshy cortex of the articulated shoots. Under the growth conditions used, *T. pergranulata* (Fig. 1A) was fast growing, having bright-green stems which were 2–3 mm in diameter (Fig. 1B), *T. indica* subsp. *indica* (from Pakistan) had thicker stems (diameter 4–5 mm) with dark- or purple-green colour (Fig. 1F), while *T. indica* subsp. *bidens* (from Australia) had thin stems with a bright-green colour (Fig. 1J), resembling *T. pergranulata*. In *T. indica* subsp. *indica*, the segments in the vegetative branches are compact with formation of a cylindrical jointed stem (Fig. 1F), in contrast to *T. indica* subsp. *bidens*, whose stems are longer and narrower towards the base, resulting in a moniliform jointed stem (Fig. 1K). Figure 1E shows plants of *T. indica* subsp. *indica* in a natural habitat in Pakistan.

All three taxa have morphology which is typical for members of subfamily Salicornioideae, including short internodes and nearly aphyllous shoots with scale-like leaves (Fig. 1). The cylindrical stem has a fleshy cortex with chlorenchyma on the periphery, which is characteristic of all species in the subfamily. Sunken anomocytic stomata are mostly distributed in vertical rows on the epidermis of the fleshy cortex of the segments, alternating with rows of cells without stomata, with their long axis oriented perpendicular to the axis of the stem (Fig. 1C, H, L, M, light bands, and D, I). In all species, stomata are located throughout the epidermis of the fleshy cortex of the segment and leaf, but they are absent in the transparent leaf marginal area and on the abaxial

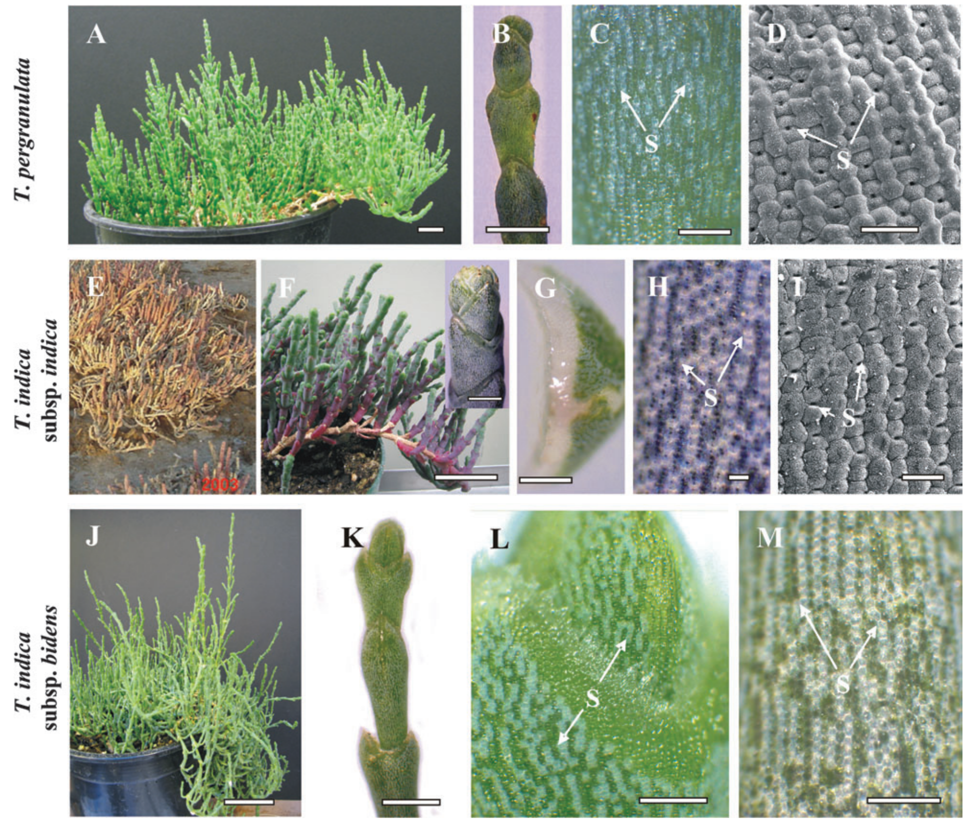

Fig. 1. General view of plants of *Tecticornia pergranulata* (A–D) and *T. indica* (E–I, subsp. *indica* and J–M, subsp. *bidens*), and characteristics of stems and their surfaces. Except for E, all images are from plants grown in WSU growth chambers. *Tecticornia pergranulata*: (A) plant ~3 months old. (B) Branch. (C) Stem surface. Light bands show the position of stomata. (D) Stem surface (SEM), showing the position of stomata. *Tecticornia indica* subsp. *indica*: (E) natural habitat. (F) Plant ~3 months old; the insert is the tip of a branch. (G) Leaf, view from the top (apical part up, abaxial side to the right). (H) Stem surface with light bands showing the position of stomata. (I) Stem surface, SEM. *Tecticornia indica* subsp. *bidens*: (J) plant ~3 months old. (K) Branch. (L) Tip of the branch. (M) Stem surface. Light bands show the position of stomata. S, stomata. Scale bars: 1 cm for A; 3 mm for B, F (inset), K; 5 cm for F, J; 1 mm for G; 0.5 mm for C, L, M; 100 μm for D, H, I.

epidermis along the leaf main rib (Fig. 1F, G, K, L). In C_4 *T. indica*, stomata are located only in the epidermal cells which are external to the groups of chlorenchyma cells (Fig. 2K).

Light microscopy

The stem tissue of *T. pergranulata* has C_3 anatomy, with two layers of mesophyll chlorenchyma surrounding the periphery of the cortex with WS tissue in the centre (Fig. 2A–D). In the reduced leaves of *T. pergranulata*, the chlorenchyma tissue occurs only on the abaxial side (results not shown, but similar to that of *Salicornia fruticosa*; see Fahn and Arzee, 1959).

In the stems of *T. pergranulata*, most of the peripheral vascular bundles are located in WS tissue one cell apart from the chlorenchyma cells, and they are distributed with the phloem facing towards the chlorenchyma, with the central cylinder in the centre of the stem. There are large intercellular air spaces beneath the stomata (also see Carolin *et al*., 1982). In this species, chlorenchyma tissue comprises ~35% and WS tissue ~60% of the total area of stem cross-section. Starch grains are abundant throughout all chlorenchyma cells, with the highest density in the outermost layer (Fig. 2D).

In both subspecies of *T. indica*, analysis of cross-sections of the young shoot segments showed that the main volume of fleshy cortex is comprised of WS tissue (Fig. 2E, L). In subspecies *indica* (Fig. 2E), the peripheral chlorenchyma tissue is 15–20% while the WS parenchyma is 70–75% of the total area of the stem cross-section. In *T. indica* subsp. *bidens* (Fig. 2L), the stems are thinner, and the tissue in the chlorenchymatous rings is 20–30% of the total area of the stem segment (depending on the position of the section from the node). As in *T. pergranulata*, chlorenchyma tissue occurs only on the abaxial side of the reduced leaves in both subspecies of *T. indica* (Fig. 2M). In the stems of *T. indica*, small peripheral vascular bundles are distributed directly under the bundle sheath cells (BSCs).

Both subspecies of *T. indica* have two layers of chlorenchyma, which are characteristic of C_4 species with Kranz anatomy, an outer layer of palisade MCs and an

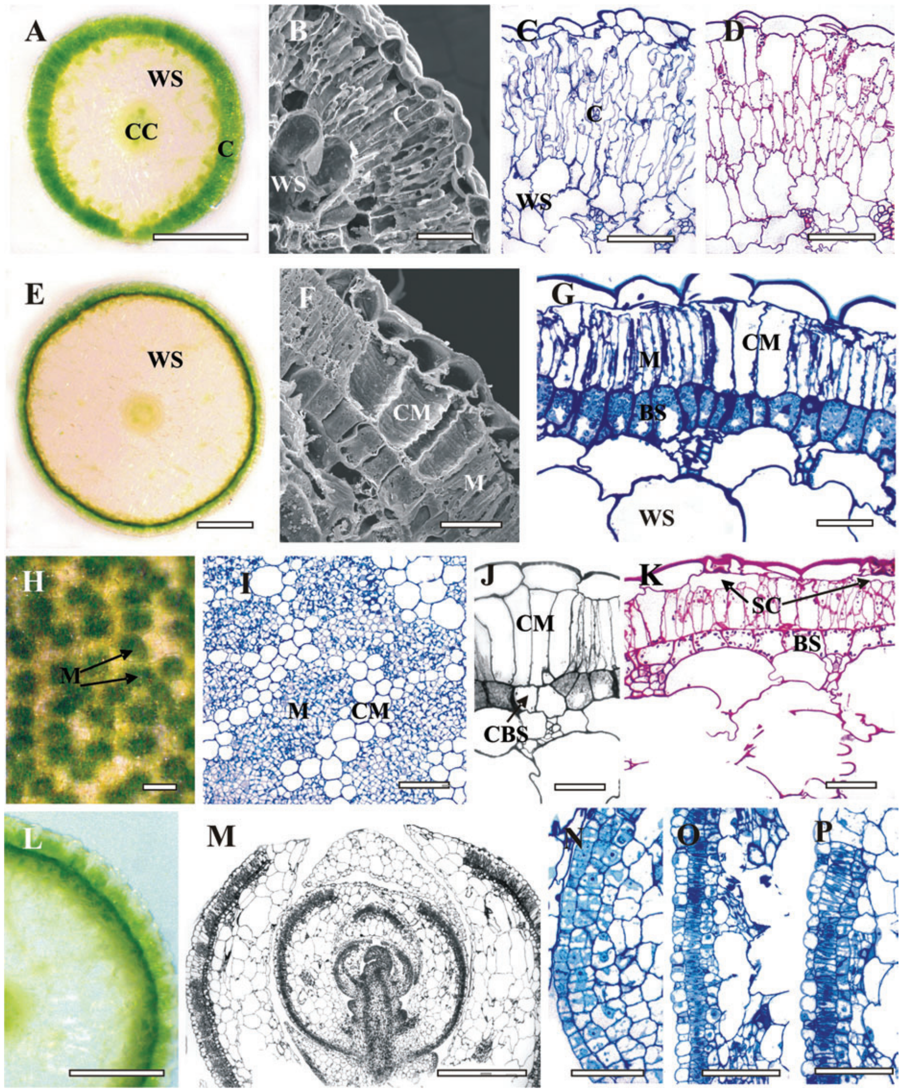

Fig. 2. Hand-cut sections (A, E, H, L), SEM (B, F), general anatomy (C, G, I, J, M–P), and periodic acid–Schiff's (PAS) staining procedure for carbohydrates (D, K) of stems of *T. pergranulata* (A–D) and *T. indica* (E–K subsp. *indica* and L–P subsp. *bidens*). (A–G, J–L) Cross-sections of the stems. (D, K) PAS staining for carbohydrates showing starch localization. (H) Hand-cut section and (I) resin-embedded paradermal section of the stem showing the distribution of the chlorenchyma and colourless cells. (M) Longitudinal section of the tip of the shoot showing the positioning of the chlorenchyma only along the abaxial side of the leaf and its absence on the adaxial side and along the leaf tip. (N–P) Longitudinal sections of a young segment showing the development of chlorenchyma from the base (N) through the middle (O) to the tip of the leaf (P). BS, bundle sheath cells; C, chlorenchyma; CBS, colourless bundle sheath cells; CC, central cylinder; CM, colourless mesophyll; M, mesophyll cells; SC, substomatal cavity; WS, water storage tissue. Scale bars: 1 mm for A, E; 100 μm for B–D, H, N–P; 50 μm for F, G, I, J, K; 0.5 mm for L, M.

inner layer of BSCs (Fig. 2E–G, J, L). The unusual feature of these species is the presence of large colourless MCs separating groups of chlorenchymatous palisade MCs (Fig. 2F–I, L). Observations of paradermal sections show that the islands of chlorenchyma cells are surrounded by a network of large colourless MCs which consist of 1–3 cells across (Fig. 2H, I). In hand-cut paradermal sections, it was also noticed that there is no green colour in BSCs in some regions where there are colourless MCs between the chlorenchyma cells (Fig. 2H). More careful studies showed that there are sparse, nearly empty cells in the layer of BSCs which are located under colourless MCs (Fig. 2J); colourless BSCs were observed more often in *T. indica* subsp. *indica*. The colourless BSCs located under groups of colourless MCs appear to have no, or limited, contact with the neighbouring chlorenchymatous MCs. There are rather large intercellular air spaces between the epidermal and chlorenchyma cells beneath the stomata (substomatal cavity), while between stomata the MCs are closely associated with epidermal cells (Fig. 2J, K). Larger intercellular air spaces also occur between the distal ends of MCs in both subspecies of *T. indica*; whereas, at the proximal ends, all MCs are close to each other with little or no intercellular air space, depending on the subspecies studied: in subsp. *bidens* there are more intercellular air spaces where the bundle sheath (BS) CW faces the MCs, and, in general, cells are more tightly packed in subsp. *indica*. Starch granules are abundant in BSC chloroplasts of both subspecies (results shown only for subsp. *indica*, Fig. 2K).

Development of the two-layered chlorenchyma tissue in *T. indica* subsp. *bidens* is shown in the longitudinal section of the shoot tip (Fig. 2M) and the young segment (Fig. 2N–P). Both layers of photosynthetic cells evidently originate from one layer of pre-chlorenchyma cells during leaf development (Fig. 2M) and during formation of the cortex chlorenchyma in the internodal meristem (Fig. 2N). In the outer row of chlorenchyma, there are cells with different levels of development, with some having a lower cytoplasmic content which could be distinguished at a rather early stage (Fig. 2O, P). Presumably, these cells with lower cytoplasmic content are precursors to the formation of the colourless MCs.

Fluorescence of chloroplasts and cell walls, and lignification

For all three representative taxa, fresh hand-cut sections placed in water have red fluorescence from chloroplasts in the outer chlorenchyma layers, with lower intensity red fluorescence coming from the pith, and from parenchyma tissue between the central cylinder and a suberized layer (which is considered periderm, e.g. see Discussion, and Arcihovskii, 1928; Vosnesenskaya and Steshenko, 1974). In all three taxa there was very bright blue fluorescence of CWs under UV light (Fig. 3A, D, G). Since it is known that lignified and suberized CWs have bright blue fluorescence, the sections were treated with phloroglucinol to test for lignification; the results are shown in Fig. 3B, E, H. Staining with phloroglucinol changed the colour of xylem, sclerenchymatous tissue, and mechanical extraxylary fibres to dark red, showing the presence of lignification only in these tissues (Fig. 3B, E, H). The blue fluorescing CWs of WS tissue did not change their colour. Several cell layers outside the central cylinder, having especially bright light-blue fluorescence in sections placed in water, changed their colour slightly to red with phloroglucinol treatment. Staining of sections with Sudan IV changed the colour of CWs outside the central cylinder to dark red, showing the presence of suberin (not shown). Thus, the blue fluorescence of CWs of WS and other cells is not related to lignification or suberization in these species.

Sections were then treated with NH_4OH to check for the presence of bound ferulic acid. In all three representatives, under alkaline conditions the blue fluorescence of all non-lignified CWs became more intense and changed colour to green, demonstrating the presence of CW-bound ferulic acid. In contrast, the colour of CWs of all xylem vessels in the central cylinder and in small vascular bundles, sclerenchymatous tissue in the central cylinder, and rare mechanical fibres outside the suberized layer remained bright blue under alkaline conditions (Fig. 3C, F, I), indicative of lignified or suberized CWs.

In all three *Tecticornia* representatives, the most intensive blue fluorescence of CWs in sections in water was in the epidermis, WS tissue, the 2–3 layers of thick-walled peridermal cells outside the central cylinder, and mechanical tissues surrounding vascular bundles, together with the xylem (Fig. 3A, D, G). Furthermore, in both C_4 subspecies, BS and colourless mesophyll CWs fluoresce more intensively than chlorenchymatous mesophyll CWs. Morphometrical study of CW thickness showed that all three taxa have a rather thick outer epidermal CW, which was thickest in *T. indica* subsp. *indica* (Table 1). Chlorenchyma MCs have thin CWs (~0.07–0.08 μm) in all three representatives. BSCs of both *T. indica* subspecies have rather thick CWs (~0.8 μm in subsp. *indica* and ~0.5 μm in subsp. *bidens*). The thickness of CWs in WS tissue and colourless MCs is similar to the thickness of BS CWs for both *T. indica* subspecies, with greater thickness in subsp. *indica*. The thickness of the CW in WS tissue in *T. pergranulata* is also more than twice that of the mesophyll CW, but much lower than in the two subspecies of *T. indica* (Table 1). Thus, the higher fluorescence in the CW of the outer epidermal, BS, and WS tissue appears related to the greater thickness of CW in these tissues.

Electron microscopy

Stems of all three *Tecticornia* taxa are covered by a thick cuticle which has a structure typical of many desert chenopods, with a rather well-formed outer lamellated layer of cuticle proper, followed by the inner cuticular layer with intensive development of reticulated polysaccharide microfibrils, also called dendrites (Fig. 4A, E). The thickness of the cuticle layer depends on the age of the segment, but, in general, the thickest cuticle was found in *T. indica* subsp. *indica* (~2 μm) while the other two taxa, *T. pergranulata* and *T. indica* subsp. *bidens*, have rather similar cuticle thickness of ~0.7 μm (Table 1). The thickness of the outer epidermal CW varies from 1.1 μm in *T. indica* subsp. *bidens*, to 1.7 μm in *T. pergranulata*, to 3 μm in *T. indica* subsp. *indica* (Table 1).

In chlorenchyma cells of *T. pergranulata*, the chloroplasts, which are located mostly towards the intercellular spaces, have grana consisting of 8–10 thylakoids (Fig. 4B). Mitochondria are rather small (~0.4 μm, Table 2), and have falciform cristae, which is typical for C_3 species. MCs have a thin CW, 0.08 μm (measured between two adjacent MCs divided by 2, Table 1), which is similar to that measured at the intercellular air space (not shown).

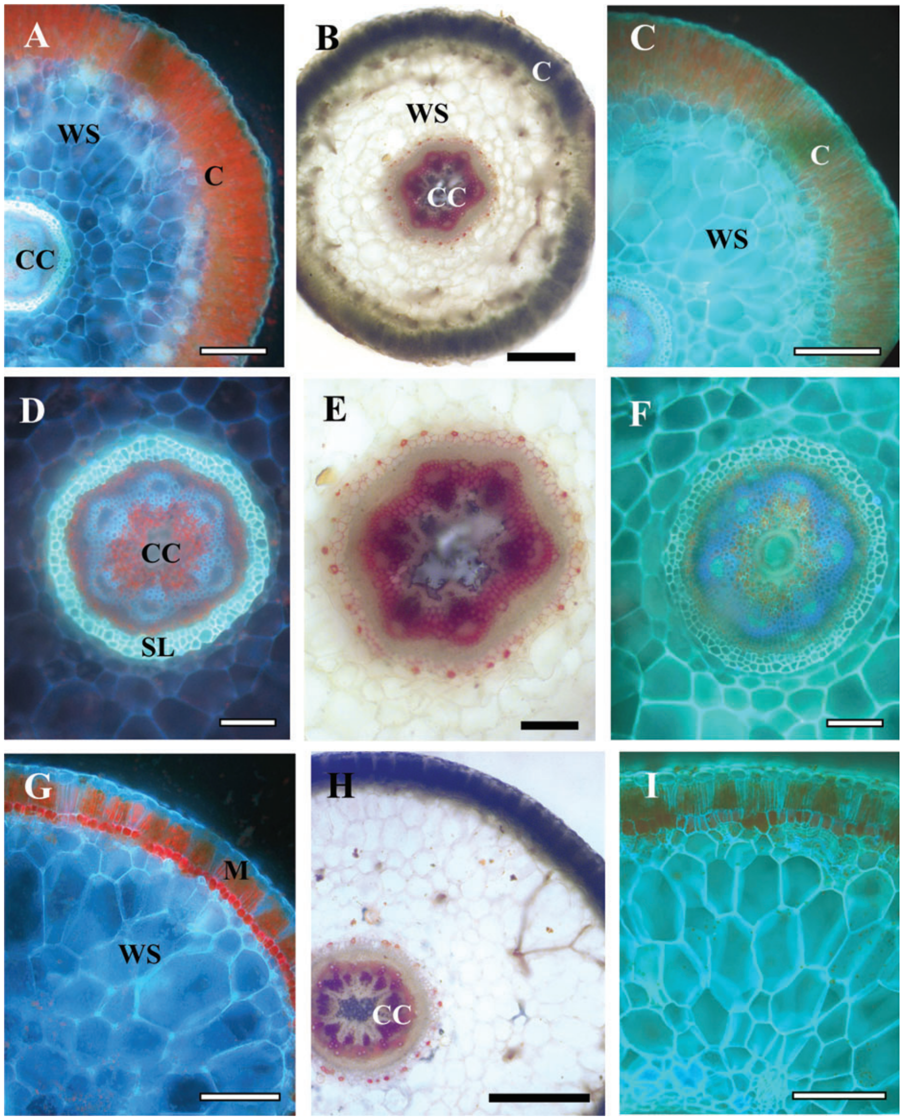

Fig. 3. Blue-green fluorescence under UV light and lignification in the hand-cut cross-sections of *T. pergranulata* (A–F) and *T. indica* subsp. *indica* (G–I). (A, D, G) Blue autofluorescence of the CW in fresh sections placed in water. (B, E, H) Staining with phloroglucinol changes the colour of mechanical tissues and xylem to dark red, showing the presence of lignified CWs. (C, F, I) Light-green fluorescence of CWs in sections placed in 0.1 M NH_4OH. C, chlorenchyma; CC, central cylinder; M, mesophyll cells; SL, suberized layer; WS, water storage tissue. Scale bars: 350 μm for A and C; 500 μm for B and H; 150 μm for D–F; 200 μm for G and I.

Table 1. *Thickness of the cuticle and cell walls in* Tecticornia *species (μm)*

Analyses were made by one-way ANOVA with Tukey's HSD. Means followed by a different lower-case letter within a row indicate a significant difference between cell types ($P \leq 0.05$). Means followed by a different upper-case letter within a column indicate a significant difference between species ($P \leq 0.05$).

Species		Cell wall				
	Cuticle	Outer epidermal	Chlorophyllous mesophyll[a]	Colourless mesophyll[a]	Bundle sheath[a]	Water storage[a]
T. pergranulata	0.65±0.04 A	1.71±0.04 Aa	0.08±0.01 Ab	–	–	0.19±0.01 Ac
T. indica subsp. *indica*	2.18±0.07 B	3.07±0.18 Ba	0.07±0.01 Ab	0.73±0.06 Ac	0.75±0.11 Ac	0.75±0.03 Bc
T. indica subsp. *bidens*	0.74±0.01 A	1.14±0.08 Aa	0.08±0.01 Ab	0.34±0.02 Bc	0.52±0.02 Bd	0.26±0.01 Ce

[a] The thickness of two adjacent cell walls was measured and divided by 2. The average number of partial cell profiles/sections examined was 29.

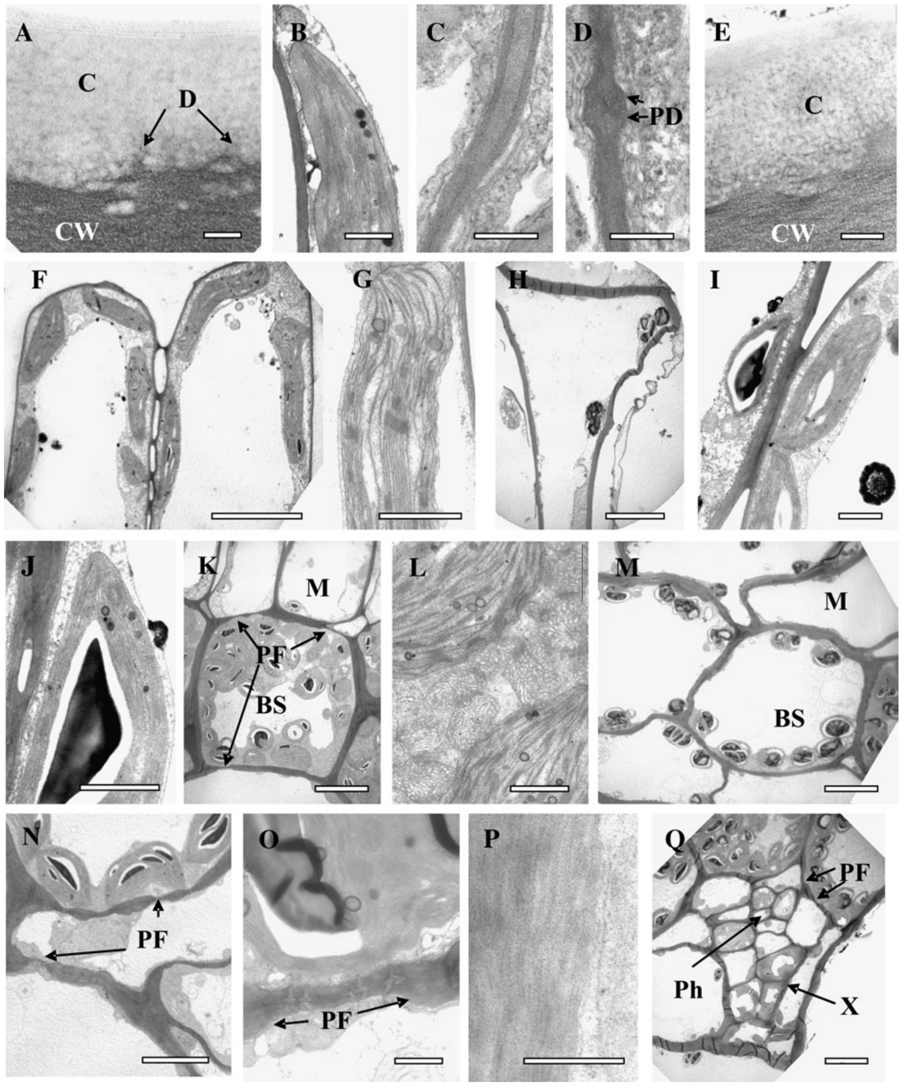

Fig. 4. Electron microscopy of cuticle, CWs, chloroplasts, and mitochondria in chlorenchyma cells in stems of *T. pergranulata* (A–D) and *T. indica* subsp. *indica* (E–I). (A, E) Cuticle. (B) Mesophyll chloroplast. (C, D) Contact of two neighbouring MC walls (C) with thickened area with plasmodesmata (D). (F, G) General view of an MC (F) and mesophyll chloroplast with reduced grana (G). (H) Colourless MCs with thickened CWs and starch-accumulating chloroplasts. (I) Comparison of chloroplast structure in colourless MCs (to the left) and chlorenchyma MC chloroplasts (to the right). (J) Structure of a chloroplast in colourless MCs. (K) Positioning of organelles in BSCs. (L) Organelles in BSCs: numerous specialized mitochondria between granal chloroplasts. (M) Colourless BSCs with starch-accumulating chloroplasts. (N, O) Plasmodesmata in the inner BS CW towards the vascular bundle parenchyma (N) and WS tissue (O). (P) Undulating positioning of cellulose microfibrils in a thickened CW between colourless MCs and BSCs. (Q) Positioning of a vascular bundle facing the phloem side towards the BSC. C, cuticle; BS, bundle sheath cell; D, dendrites (polysaccharide microfibrils); M, mesophyll cell; PD, plasmodesmata; PF, pit field; Ph, phloem; X, xylem. Scale bars: 0.2 μm for A and E; 0.5 μm for B–D and P; 1 μm for G, I, J, L and O; 5 μm for F and N; 10 μm for H, K, M, and Q.

Very often, two neighbouring mesophyll CWs are not very tightly appressed to each other, having the intercellular space filled with fibrillar material (Fig. 4C). Plasmodesmata are more often found in the tangential (periclinal) CW between two MCs rather than in the radial (anticlinal) CW; but, in both cases, they are located in the local thickening of the CW (Fig. 4D). All WS cells are interconnected by plasmodesmata, which are also located in a thickened area of the CW (not shown).

The ultrastructure of palisade MCs and Kranz BSCs in both subspecies of *T. indica* is similar in general features. The chloroplast size (based on length) in the chlorophyllous and colourless MCs and BSCs is ~4–6 μm, with little to no difference in size between the cell types, and from that in MCs of *T. pergranulata*. The thylakoid system in the mesophyll chloroplasts consists of sparse grana which have short thylakoids with a high degree of stacking and numerous, long intergranal thylakoids (Fig. 4G, subsp. *indica*). Mesophyll mitochondria in the two subspecies are rather small (~0.4 μm) and comparable in size with mitochondria in MCs of *T. pergranulata* (Table 2). MCs usually are packed rather tightly on their

Table 2. *Size of mitochondria and chloroplasts in* Tecticornia *species (μm)*

Analysis was by one-way ANOVA with Tukey's HSD. Means followed by a different lower-case letter within a row indicate a significant difference between cell types; comparison was made independently for chloroplast and mitochondria sizes ($P \leqslant 0.05$). Means followed by a different upper-case letter within a column indicate a significant difference between species ($P \leqslant 0.05$). The average number of organelle sections examined in each case was 35 for chloroplasts and 20 for mitochondria. M, mesophyll, BS, bundle sheath.

Species	Chloroplast length			Mitochondria small diameter			
	Chlorophyllous M	Colourless M	BS	Chlorophyllous M	Colourless M	BS	Colourless BS
T. pergranulata	4.98±0.12 A	–	–	0.36±0.03 A	–	–	–
T. indica subsp. *indica*	5.05±0.18 Aa	5.08±0.29 Aa	5.82±0.21 Aa	0.38±0.02 Aa	0.39±0.02 Aa	0.57±0.02 Ab	0.41±0.01 Aa
T. indica subsp. *bidens*	6.23±0.15 Ba	3.94±0.31 Bb	5.22±0.11 Ac	0.40±0.02 Aa	0.32±0.02 Aa	0.58±0.02 Ab	0.63±0.01 Bc

proximal end in *T. indica* subsp. *indica*, while subsp. *bidens* often has small air spaces between MCs and BSCs. As in the C_3 *T. pergranulata*, MCs in both subspecies have rather thin CWs, ~0.07–0.08 μm (Table 1), while the CW thickness in BSCs is 10 times higher for subsp. *indica* and ~7 times higher for subsp. *bidens*. Colourless MCs have obviously thicker CWs than chlorenchyma MCs (Fig. 4H, I), up to 10 times in subsp. *indica* and four times in subsp. *bidens* (see Table 1). The colourless MCs have plasmodesmata connections with neighbouring cells: MCs, other colourless MCs, BSCs, and colourless BSCs. These cells contain a few chloroplasts which are filled with starch (Fig. 4I, J), and small mitochondria which are comparable in size and internal structure with mesophyll mitochondria (the size of mitochondria in both MCs and colourless MCs is ~0.4 μm, Table 2). The Kranz cells have preferentially centrifugally arranged chloroplasts in both subspecies (Figs 2G, 4K), with numerous, well-developed irregular grana interconnected by intergranal thylakoids (Fig. 4L). Specialized mitochondria are located between chloroplasts in the distal part of the cell or along the thinner cytoplasmic layer in the inner (proximal) part of the BSC (Fig. 4L). The BS mitochondria are ~50% larger than the MC mitochondria in both subspecies (Table 2), and they have mostly tubular cristae, with only some of them having a lamelliform appearance (Fig. 4L). Thick BS CWs are penetrated with pit fields on the border with MCs and between neighbouring BSCs, and also in the inner tangential CW between BSCs and WS cells (Fig. 4N, O). Colourless cells in the BS layer are similar to the chlorenchymatous Kranz BSCs in having thick CWs and pit fields with plasmodesmata. They differ from the Kranz cells by containing only a few chloroplasts with large starch grains and sparse mitochondria in a rather thin cytoplasmic layer (Fig. 4M). Colourless BSCs appear to be located internal to groups of colourless MCs. In the two subspecies, the CW of WS tissue is also much thicker than that of the chlorophyllous MCs (Table 1). In subsp. *indica*, the thickness of the CW of WS cells is comparable with that of BSCs and colourless mesophyll CWs, while in subsp. *bidens*, the WS CWs are about half as thick as BS CWs and similar in thickness to CWs of colourless MCs (Table 1). The thick CWs in WS parenchyma, colourless MCs and BSCs have a similar undulated distribution of cellulose microfibrils (Fig. 4P), which is not observed in other tissues. In WS tissue, the cells are interconnected with plasmodesmata, which are located in a thickened area of the CW (not shown, but similar to that in Fig. 4D). As noted earlier, the small peripheral bundles are often directly adjacent to BSCs, and one of the most interesting features of this genus is that the phloem side of the bundles is facing chlorenchyma tissue (Fig. 4Q).

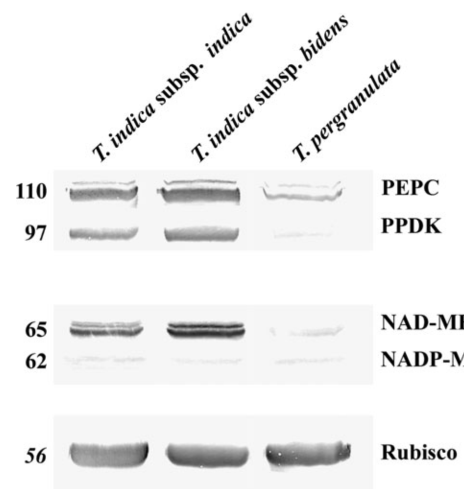

Fig. 5. Western blots for C_4 enzymes and Rubisco from total proteins extracted from green shoots of *T. pergranulata*, and *T. indica* subsp. *indica* and subsp. *bidens*. Blots were probed with antibodies raised against PEPC, PPDK, NAD-ME, NADP-ME, and Rubisco, respectively. Numbers on the left indicate the molecular mass in kilodaltons. Western blots were replicated a minimum of three times with each antibody with similar results.

Western blots

SDS–PAGE blots of total proteins extracted from leaves were probed immunologically to test for C_4 enzymes and Rubisco LSU (Fig. 5). The molecular masses of the immunoreactive bands corresponded to the expected mass of the different polypeptides. The results show a strong immunoreactive band for Rubisco LSU at 56 kDa in all species. Strong immunoreactivity was observed for PEPC and PPDK in the two C_4 subspecies. With antibodies to C_4 acid decarboxylases, there was immunolabelling for NAD-ME (65 kDa) in both subspecies of *T. indica*, with extremely low labelling for NADP-ME (62 kDa) (Fig. 5), and no labelling for PEP-CK in any of the species (not shown). In the C_3 species *T. pergranulata*, there were very low immunoreactive bands for all C_4 enzymes, i.e. PEPC, PPDK, NAD-ME, and NADP-ME (Fig. 5), and no labelling for PEP-CK (not shown).

Immunolocalization of enzymes and starch distribution

In the C_3 species *T. pergranulata*, immunolabelling for Rubisco occurs in chloroplasts of all chlorenchyma cells (Fig. 6A), similar to the distribution of starch grains (Fig. 2D). The distribution of *in situ* immunolabelling for several photosynthetic enzymes in the C_4 *T. indica* subsp. *indica* is shown at light microscopy (Fig. 6B, C) and electron microscopy levels (Fig. 7) (also see Table 3 for comparison of the density of labelling for different photosynthetic enzymes in different cell types for the two subspecies). There was strong labelling for Rubisco LSU in chloroplasts in BSCs (Fig. 6B, Table 3) which also store starch (Fig. 2K), and the few chloroplasts found in WS cells also show labelling for Rubisco (not shown). Labelling for PEPC is high in MCs (Fig. 6C) and is confined to the mesophyll cytosol (Fig. 7C, Table 3). Transmission electron microscopy studies of the two subspecies of *T. indica* show immunolabelling for NAD-ME and GDC in BSC mitochondria (Fig. 7B).

To study the possible function of colourless MCs, immunolabelling was performed at the electron microscopy level (see results Table 3). For both *T. indica* subspecies, the labelling for PEPC is highest in the cytosol of MCs (Fig. 7C, Table 3); however, the colourless MC also showed substantial labelling (though significantly lower than in MCs) (Fig. 7D, Table 3). Labelling for PPDK was shown to be localized predominantly in chloroplasts of MCs, with lower, but significant, labelling in chloroplasts of colourless MCs. Labelling for PPDK in BS chloroplasts and for PEPC in BS cytosol was similar to background (Table 3). Starch distribution, in general, followed the pattern of Rubisco localization, with higher starch content in BSCs in comparison with MCs, but the largest starch granules are localized in the colourless MCs and colourless BSCs in *T. indica* subsp. *indica* (Fig. 4H, J, M).

Gas exchange measurements, carbon isotope composition, and titratable acidity

Similar responses of photosynthesis to varying light were observed for the C_3 plant *T. pergranulata* and C_4 species *T. indica* subsp. *indica* and subsp. *bidens*. In all three taxa, photosynthesis saturates at relatively high light intensity, ~1200 PPFD, but *T. pergranulata* reaches a higher maximum rate than the C_4 species (Fig. 8). The rate of photosynthetic CO_2 fixation was measured at varying

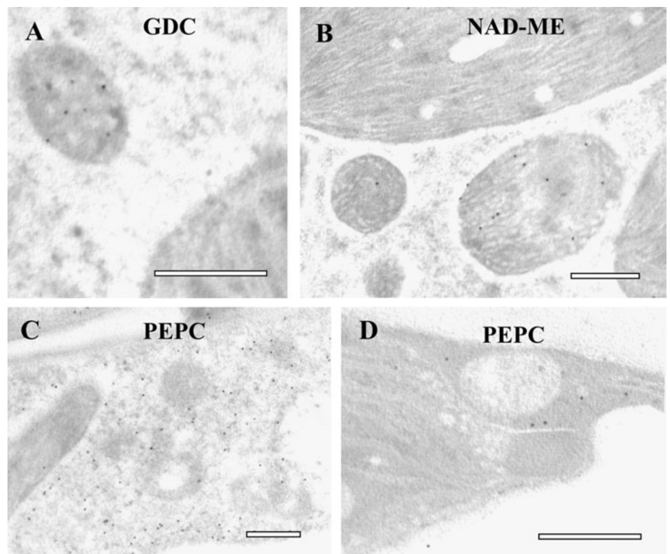

Fig. 7. Electron microscopy of *in situ* immunolocalization of PEPC, NAD-ME, and GDC in chlorenchyma cells of *T. indica* subsp. *indica*. (A) GDC and (B) NAD-ME in BSC mitochondria. Scale bars: 0.5 μm; (C, D) PEPC in chlorenchyma MC cytosol (C) and colourless MC cytosol (D).

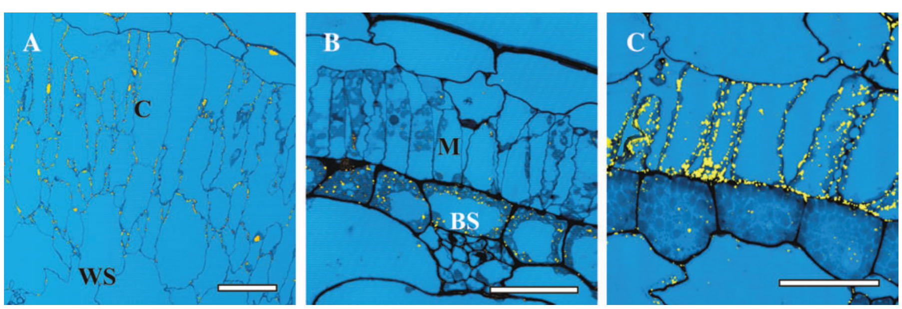

Fig. 6. Reflected/transmitted confocal imaging of *in situ* immunolocalization of photosynthetic enzymes in stems of *T. pergranulata* (A) and *T. indica* subsp. *indica (*B, C). Immunolabel appears as yellow dots. (A, B) Rubisco. (C) PEPC. Scale bars: 50 μm.

Table 3. *Cellular immunogold labelling of photosynthetic enzymes in various cells of stems of* Tecticornia indica *subsp.* indica *and subsp.* bidens *(number of gold particles per 1 μm²)*

Analysis was by one-way ANOVA with Tukey's HSD. Means followed by a different lower-case letter within a row indicate a significant difference between cell types ($P \leqslant 0.05$). For PEPC comparisons were made between numbers of particles in the cytosol of three cell types, for PPDK and Rubisco comparisons were made between the numbers of particles in chloroplasts of three types of cells. The number of gold particles is given as the mean ±SE. The average number of partial cell profiles/sections examined was 20.

Species	Chlorophyllous mesophyll cells			Colourless mesophyll cells			Bundle sheath cells		
PEPC	Organelles	Cyt	Background	Organelles	Cyt	Background	Organelles	Cyt	Background
T. indica subsp. *indica*	1.3±0.4	7.3±1.1 a	0.6±0.2	0.9±0.3	3.1±0.8 b	1.9±0.5	1.0±0.4	1.3±0.6 c	0.8±0.4
T. indica subsp. *bidens*	1.5±0.4	9.4±1.1 a	1.0±0.3	2.6±0.7	6.3±1.1 b	1.2±0.3	1.1±0.2	1.5±0.3 c	0.8±0.2
PPDK	A	B	C	A	B	C	A	B	C
T. indica subsp. *indica*	9.6±1.0 a	1.4±0.2	0.5±0.2	4.8±0.8 b	0.9±0.3	1.9±0.5	2.7±0.4 c	0.9±0.1	2.8±1.1
T. indica subsp. *bidens*	15.0±1.2 a	1.7±0.3	1.7±0.2	5.8±1.0 b	0.5±0.4	1.9±0.6	1.5±0.3 b	0.7±0.3	2.0±1.1
Rubisco	A	B	C	A	B	C	A	B	C
T. indica subsp. *indica*	2.8±0.4 a	0.06±0.03	0.3±0.1	4.7±0.7 a	0.2±0.1	0.7±0.2	20.8±1.3 b	0.2±0.1	0.4±0.03
T. indica subsp. *bidens*	4.1±0.5 a	0.35±0.2	0.4±0.3	11.3±1.0 b	0.4±0.2	0.4±0.2	22.8±2.1 c	0.2±0.1	0.4±0.2

A, Chloroplast; B, Cyt + other organelles; C, Background.

intercellular levels of CO_2 (C_i) under atmospheric (21%) and low (2%) concentrations of O_2. Under varying CO_2 and ambient O_2, the C_3 species *T. pergranulata* has lower carboxylation efficiency, and increasing rates of CO_2 fixation up to a C_i of 900 μmol mol^{-1} (Fig. 9A), whereas the two Kranz-type subspecies show a similar, relatively rapid increase in photosynthesis with increasing C_i up to ~600 μmol mol^{-1} (Fig. 9B, C). A higher level of O_2 was inhibitory for photosynthesis rates under varying CO_2 in *T. pergranulata* (Fig. 9A), while both *T. indica* subspecies had no inhibition of photosynthesis by O_2 (Fig. 9B, C). The Γ* was determined for the three taxa (Table 4) by analysis of the intercept of CO_2 response curves at different light intensities (as illustrated in Fig. 9D for *T. indica* subsp. *bidens*). Γ* is much lower in the Kranz-type C_4 species than in the C_3 species. Both *T. indica* subspecies have C_4-type $\delta^{13}C$ values (subsp. *indica* –13.7‰, and subsp. *bidens* –15.2‰), while *T. pergranulata* has C_3-type values (–31.4‰). Titratable acidity tests did not reveal any changes in pH of cell sap during the diurnal cycle (Table 4).

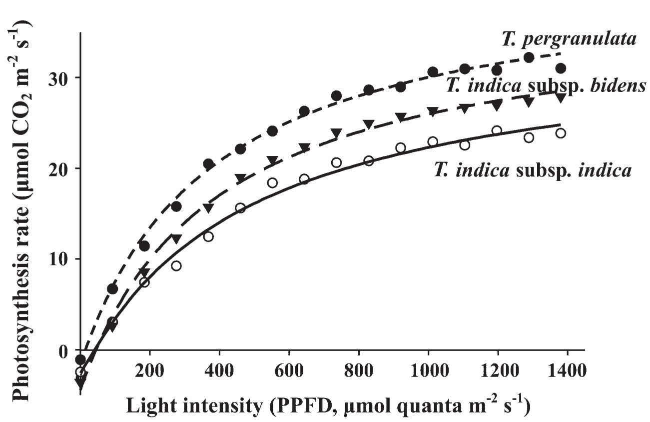

Fig. 8. Rates of CO_2 fixation in response to varying light at 25 °C and 370 μmol mol^{-1} of CO_2 in *T. pergranulata*, and *T. indica* subsp. *indica* and subsp. *bidens*. The results represent the average of three replications from measurements made on different branches.

Discussion

There has been a strong interest in the evolution of C_4 photosynthesis in the family Chenopodiaceae, due to its unusually high diversity, with different Kranz and non-Kranz C_4 leaf types as well as variation in C_3 leaf types (Monteil, 1906; Carolin *et al.*, 1975; Fisher *et al.*, 1997; Jacobs, 2001; Pyankov *et al.*, 2001*a*, *b*; Schütze *et al.*, 2003; Kapralov *et al.*, 2006). *Halosarcia*, as traditionally defined, has been shown to be paraphyletic in relation to other Australian Chenopodiaceae genera (Shepherd *et al.*, 2004; Kadereit *et al.*, 2006; this study). The monophyly obtained from molecular studies has been supported based on morphological characters which show a high level of homoplasy (Shepherd *et al.*, 2005; Shepherd and Wilson, 2007). Because of this, these genera have all recently been reorganized into a more broadly defined *Tecticornia* (Shepherd and Wilson, 2007), which is accepted here. While this clade of species is predominantly Australian in distribution, it is also found on other continents, including southern Asia (Malaysia, Sri Lanka, India, and Pakistan) and tropical East Africa along coastal and inland saline areas. Interestingly, the only species previously described as having C_4 photosynthesis, *T. indica*, is also one of the few Australian chenopod lineages also to be found outside of the continent. Carolin *et al.* (1982) identified four subspecies of *Halosarcia* (= *Tecticornia*) *indica* (*bidens*, *indica*, *julacea*, and *leiostachya*) as C_4 plants. From molecular phylogeny based on nuclear DNA internal transcribed spacer (ITS) data, *T. indica* and most of its subspecies form a strongly supported clade with undescribed entities previously

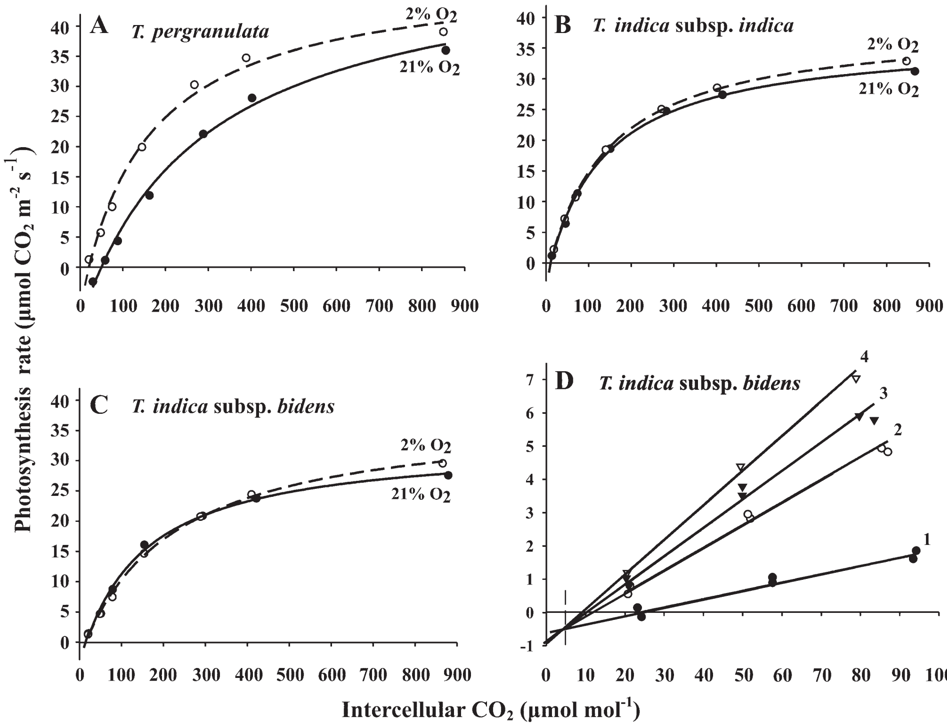

Fig. 9. Rates of CO_2 fixation in response to varying intercellular levels of CO_2 at 25° C and 900 PPFD in *T. pergranulata* (A), *T. indica* subsp. *indica* (B), and subsp. *bidens* (C). The results represent the average that was taken of ambient to low CO_2 response, and ambient to high CO_2 response, from separate measurements on 2–3 branches. (D) Illustration of calculation of Γ^* from CO_2 response curves at 25 °C under four light intensities with *T. indica* subsp. *bidens*: 90 (line 1), 170 (line 2), 260 (line 3), and 360 (line 4) PPFD. Each light level is the response to two replications.

Table 4. *CO_2 compensation point, carbon isotope discrimination ($\delta^{13}C$), and test for CAM in* Tecticornia *species*

For determination of Γ^* see Fig. 9. For $\delta^{13}C$ and titratable acidity n=2.

Species	Γ^* (μmol mol^{-1})	$\delta^{13}C$ (‰)	Titratable acidity (μeq g FW^{-1})		
			End of the night	Middle of the day	End of the day
T. pergranulata	34.2	–31.4±0.05	1.82±0.23	1.93±0.04	1.96±0.08
T. indica subsp. *indica*	5.2	–13.7±0.01	2.42±0.57	2.97±0.53	2.50±0.13
T. indica subsp. *bidens*	4.8	–15.2±0.01	3.99±0.10	4.01±0.09	3.66±0.21

referred to as 'Yanneri Lake' (Shepherd and Wilson, 2007), which has been suggested also to be C_4 (K Shepherd, personal communication). This may indicate a single origin of C_4 photosynthesis in Salicornioideae. However, *T. indica* subsp. *julacea* is not part of the *T. indica* clade in the ITS tree (Kadereit *et al*., 2006), only in the chloroplast DNA *trnL* tree of Shepherd *et al*. (2004). The phylogenetic positions of the C_3 and C_4 taxa utilized in this study were verified by comparison with some other species in genus *Tecticornia* and related genera in subfamily Salicornioideae using ITS as a marker and maximum likelihood analysis (Fig. S1 and Table S1 in Supplementary material available at *JXB* online). Obviously, a more detailed analysis of *T. indica* subspecies is needed. The differences between two subspecies of *T. indica*, subsp. *indica* and subsp. *bidens*, including their different habit (subsp. *indica* is a prostrate dwarf shrub up to 50 cm, rarely to 1 m, versus subsp. *bidens* which is an erect shrub up to 2 m tall) (Wilson, 1980), macroscopic, microscopic, and genetic differences described in this paper, and their different geography, collectively support specifically different entities. This needs to be clarified in the re-evaluation of the taxonomic status of this complex in a broad geographical context. These results, and a similar case already discussed in the genus *Bienertia* (Akhani *et al*., 2005), indicate that the taxonomy of several critical groups of Chenopodiaceae needs to be reassessed using multidisciplinary approaches.

Anatomical features

The structure of chlorenchyma in C_3 *T. pergranulata*, consisting of two layers of elongated MCs around the periphery of cylindrical leaves or aphyllous stems, is rather typical for different C_3 representatives of Salicornioideae and Salsoloideae; in aphyllous species, small reduced scale-like leaves have similar chlorenchyma tissue only on their abaxial side. This type of structure, with a peripheral position of chlorenchyma and a network of small vascular bundles, and a central cylinder (in stems) or main vascular bundle (in leaves) in the centre, has been called 'centric' (Metcalfe and Chalk, 1950), 'sympegmoid' (Carolin *et al*., 1975), or 'arco-vascular' (Vasilevskaya and Butnik, 1981). It has also been described in Salsoloideae as having peripheral vascular bundles with the xylem side facing the chlorenchyma (Carolin *et al*., 1975; also see figs 7, 8 and 11, 12 in Pyankov *et al*., 1997; fig. 2C, D in Voznesenskaya *et al*., 2001; figs 2, 5, 7 in Voznesenskaya *et al*., 2003). Although not perfect, this is a convenient way of identifying this anatomical type when it occurs, and we consider that the term 'centric' reflects well all features of C_3 anatomy in these cases. The characteristic feature distinguishing *T. pergranulata* from C_3 Salsoloideae species which have a similar structure is the positioning of peripheral vascular bundles. In *Tecticornia*, the phloem side of the small peripheral bundles faces towards the chlorenchyma tissue. Also, all peripheral bundles in C_3 *T. pergranulata* are separated from the chlorenchyma tissue by one layer of large WS cells, while in C_3 or C_3–C_4 *Salsola* species, the peripheral vascular bundles are separated from chlorenchyma cells by rather small parenchyma cells representing parenchymatous BS around peripheral vascular bundles (Pyankov *et al*., 1997; Voznesenskaya *et al*., 2001; Akhani and Ghasemkhani, 2007; EV Voznesenskaya, unpublished results). In other species of the Australian Salicornioideae such as *Tecticornia* s. str. and *Pachycornia* and *Sarcocornia*, many of the vascular bundles are adjacent to chlorenchyma (Carolin *et al*., 1982). While species in the genus *Salicornia* have a similar positioning of the phloem to that in *Tecticornia*, the peripheral bundles are often adjacent to the chlorenchyma tissue (personal observation of EV Voznesenskaya and NK Koteyeva, unpublished results). The structure and position of peripheral vascular bundles in C_3 *T. pergranulata* represent a rather distinctive feature, which may also be characteristic for some other Salicornioideae. Accepting this type of anatomy as C_3 centric, as a minimum two variants should be mentioned according to the positioning of peripheral vascular bundles.

In the two C_4 subspecies of *T. indica*, chlorenchyma tissue consists of two cell layers, elongated MCs and roundish BSCs, on the periphery of the stems and rudimentary leaves. The present observation of paradermal sections revealed that the islands of chlorenchyma cells are surrounded by sections of large, colourless MCs with thick CWs, which consist of one to three cells across, as previously reported (Carolin *et al*., 1982). Kadereit *et al*. (2003) distinguished the anatomical type in *T. indica* as Kranz-halosarcoid, based on the presence of colourless MCs and the centrifugal position of chloroplasts in BSCs. An additional distinguishing anatomical feature of this Kranz type is the position of peripheral vascular bundles directly adjacent to BSCs, with the phloem facing the chlorenchyma tissue, as was also observed in C_3 *T. pergranulata*. This differs from salsoloid-type C_4 species, where the xylem in the peripheral vascular bundles faces the chlorenchyma tissue (see Olesen, 1974; Voznesenskaya, 1976*a*, *b*; figs 7, 8, 11, 12 in Pyankov *et al*., 1997; fig. 2A, B in Voznesenskaya *et al*., 2001; figs 2, 5, 7 in Voznesenskaya *et al*., 2003). Interestingly, a similar positioning of peripheral vascular bundles, with their phloem side towards the chlorenchyma, was only previously mentioned in the 'single-cell functioning' C_4 species, *Suaeda* (=*Borszczowia*) *aralocaspica* (Freitag and Stichler, 2000). It was thought (Olesen, 1974) that such positioning of vascular bundles could facilitate the transport of assimilates and water, but this idea needs further investigation. Thus, the type of chlorenchyma structure in C_4 *Tecticornia* represents a unique variation of Kranz anatomy with discontinuous chlorenchyma, interrupted by the thick-walled colourless cells in both layers, mesophyll and BS, centrifugally arranged organelles in BSCs, and positioning of peripheral vascular bundles with their phloem side to the chlorenchyma. This type of anatomy was designated Kranz-halosarcoid by Kadereit *et al*. (2003) according to the previous name of the genus, which is now changed to Kranz-tecticornoid type. In general, this type of anatomy can be described as Kranz centric discontinuous with the specific position of vascular bundles and chloroplasts in BSCs.

According to Carolin *et al*. (1982), Fahn and Arzee (1959), and Al-Turki *et al*. (2003), in all species of subfamily Salicorniodeae studied, the network of vascular bundles in the fleshy cortex is derived from the leaf bundle of the upper internode. The type of venation in reduced leaves and cortex was classified as *Salicornia-Arthrocnemum* type (Fahn and Arzee, 1959), where the descending network venation of the cortex was derived only from lateral branches of the leaf strands. The study of venation in C_3 and C_4 *Tecticornia* species also showed this type of venation and origin of peripheral bundles, with certain differences in the structure of the primary vascular system between *T. pergranulata* and *T. indica* subsp. *bidens*; in general, the *Salicornia-Arthrocnemum* type of venation was suggested to be more advanced in comparison with venation in *Kochia-Bassia* or *Rhagodia-Atriplex* types (Bisalputra, 1962). There has been an extensive discussion of the origin of the fleshy cortex in articulated Chenopodiaceae species (see Fahn and Arzee, 1959). From examination of the origin of the cortex during plant development, it was concluded that the assimilating cortex is not a product of leaf fusion and adnation to the stem, but rather is a result of simultaneous growth of the leaf basis and cortex. It was shown that the development of the reduced leaves in species with such shoots is similar to that of ordinary foliar leaves (Vasilevskaya, 1955; Werker and Fahn, 1966) and that the fleshy tissue external to the central cylinder of these plants develops as a result of intercalary growth at the base of each internode and should be regarded as true cortex (Vasilevskaya, 1955; Fahn and Arzee, 1959). The relationship between positioning of the small peripheral bundles and transport of assimilates in different Chenopodiaceae species needs additional study.

It is interesting to note that chenopods with a fleshy cortex have a special form of secondary growth and periderm formation which was previously studied in the genus *Haloxylon*. The secondary cambium, as well as the peridermal cambium, originates in the pericycle, which is internal to the endoderm, and usually after formation of the periderm the outer fleshy chlorophyllous cortex withers and dries up (Arcihovskii, 1928; Vosnesenskaya and Steshenko, 1974). While the process of secondary growth was not studied in *Tecticornia*, light microscopy images show very similar secondary growth to that in *Haloxylon*.

Tecticornia indica*: C_4 biochemical subtype and enzyme compartmentation*

The high levels of C_4 cycle enzymes PPDK, PEPC, and NAD-ME in *T. indica* are indicative of C_4 photosynthesis, as compared with the very low levels of these enzymes in the C_3 species *T. pergranulata*. Analysis by western blots for C_4 acid decarboxylases shows that *T. indica* is an NAD-ME-type C_4 species. Generally, consistent results have been obtained in subtyping C_4 species by immunodetection versus enzymatic assay of C_4 decarboxylases (Walker *et al*., 1997; Wingler *et al*., 1999; Pyankov *et al*., 2000; Voznesenskaya *et al*., 2002). Immunolocalization studies show selective compartmentation of PPDK and PEPC in MCs, and Rubisco in BSCs, in the two subspecies of *T. indica*, characteristic of C_4 plants. High levels of starch accumulate in the BSC chloroplasts compared with MC chloroplasts (see also Carolin *et al*., 1982). Also, NAD-ME and GDC are selectively localized in mitochondria of BSCs, as expected for NAD-ME-type C_4 species.

Ultrastructural features of photosynthetic tissue

The ultrastructural characteristics of chlorenchyma cells in *T. pergranulata* are typical of other C_3 species, with chloroplasts and mitochondria around the periphery of MCs. In the two C_4 subspecies of *T. indica*, there is differentiation of chloroplasts and mitochondria between MCs and BSCs. There are numerous mitochondria in BSCs which, along with chloroplasts, are predominantly located in the centrifugal position, as was also observed by Carolin *et al.* (1982) and Jacobs (2001). The mitochondria in BSCs are ~50% larger than in MCs, while the chloroplasts in the two cell types are similar in size. However, the mesophyll chloroplasts have a reduction of grana with prevalence of intergranal thylakoids compared with BS chloroplasts. The abundance of mitochondria in BSCs and the reduction of grana in mesophyll compared with BS chloroplasts are typical of NAD-ME-type C_4 species (Carolin *et al*., 1975; Voznesenskaya, 1976*a*, *b*; Gamaley, 1985; Voznesenskaya and Gamaley, 1986; Fisher *et al*., 1997).

In most NAD-ME-type C_4 species, including dicots and monocots, the chloroplasts are in a centripetal position (Gutierrez *et al*., 1974; Hattersley, 1987; Dengler and Nelson, 1999). However, there are established cases of NAD-ME-type species having BS chloroplasts in the centrifugal position. With respect to dicots, the centrifugal position of chloroplasts in BSCs of *T. indica* is similar to that found in *Suaeda* species having a schoberia leaf type with NAD-ME C_4 photosynthesis (Schütze *et al*., 2003; Voznesenskaya *et al*., 2007). This also occurs in *Trianthema triquetra*, family Aizoaceae, which has atriplicoid leaf anatomy and an unspecified biochemical subtype, but with ultrastructural features characteristic of NAD-ME species (Carolin *et al*., 1978). With respect to monocots, the centrifugal position of BS chloroplasts has been found in several NAD-ME-type species: in spp. of *Panicum* sect. Dichotomiflora, in *Eragrostis*, and in *Enneapogon* (Ohsugi *et al*., 1982; Hattersley, 1987). Whether there is functional significance to the chloroplast position, or whether it is only indicative of alternative forms of C_4, is unknown.

Many C_4 species have BSCs with thickened CWs (see Sage and Monson, 1999). Among C_4 NAD-ME species in family Chenopodiaceae, it is possible to distinguish two groups according to the thickness of their BS CWs. Most *Atriplex* and *Suaeda* species have rather thin CWs, while representatives studied from tribe Caroxyloneae with NAD-ME-type anatomy, *Climacoptera transoxana*, *Halocharis hispida*, and *Salsola rigida* (=*Caroxylon orientale*) (Akhani *et al*., 2007), have very thick BS CWs (Voznesenskaya, 1976*b*), similar to those in C_4 *Tecticornia*. The most interesting feature of BSC structure in the C_4 *T. indica* subspecies is the presence of intercellular connections by plasmodesmata, not only in the outer tangential CW (between BSCs and MCs), but also in the inner tangential CW, between BSCs and WS tissue, and between BSCs and vascular bundle parenchyma cells. This feature suggests symplastic transport of assimilates from chlorenchyma to the vascular tissue in these C_4 species. Also, in *T. indica*, the WS cells have rather thick CWs which are interconnected by plasmodesmata.

Fluorescence of chloroplasts and cell walls, and lignification

When excited by UV radiation, leaves of all plants have intensive red fluorescence from all chlorophyll-containing cells. Obviously, the most intensive red colour in sections of stems was in the chlorenchyma tissue in the outer cortex layers, with lower red fluorescence from several other chloroplast-containing parenchymatous tissues including the pith, xylem, and phloem parenchyma, and the peridermal parenchyma (the phelloderm) which is located just outside the central cylinder. Possible functions of the internal chlorophyll-containing tissues were studied in some Salicornioideae species by Redondo-Gómez *et al.* (2005).

Certain groups of green plants exhibit a genuine blue fluorescence from their CW due to accumulation of phenolic substances, especially lignins and/or suberins. In stem sections of the *Tecticornia* taxa studied, the brightest blue fluorescence was emitted from lignified fibres, sclerenchyma, and xylem elements, and from the suberized layers outside the central cylinder representing the periderm. The blue fluorescence of non-lignified CWs (i.e. those that have a negative phloroglucinol-HCl test) changes to green with increasing intensity after treatment with 0.1 M NH_4OH, indicating the presence of bound ferulic acid (Rudall and Caddick, 1994). According to previous studies, families of monocotyledons can be divided into two groups depending on the UV fluorescence behaviour of their CW and presence or absence of bound ferulic acid (Harris and Hartley, 1976; Harris and Hartley, 1980). In dicots, wall-bound ferulic acid has only been found in the order Caryophyllales, and was previously shown for eight species of family Chenopodiaceae (Hartley and Harris, 1981).

In *T. pergranulata* and *T. indica* subspecies, the non-lignified CWs of assimilating organs fluoresce blue under UV radiation and change colour to intense green after NH_4OH treatment, indicating the presence of CW-bound ferulic acid. Intense fluorescence following NH_4OH treatment was found in all three representatives and, thus, it does not depend on photosynthetic type. There was differential distribution of fluorescence intensity in different tissues, with maximum green fluorescence after NH_4OH treatment in epidermal and WS tissues. In both C_4 subspecies, the walls of BSCs fluoresce more intense green than the chlorenchymatous MCs, with the highest intensity in the thick-walled, colourless MCs. In C_3 and C_4 *Tecticornia*, the intensity of green fluorescence following NH_4OH treatment tended to correspond to CW thickness. The epidermis has very thick CWs, and the WS tissue has much thicker CWs than the MCs in both species. In the C_4 subspecies of *T. indica*, the WS tissue, BSCs, and colourless MCs have higher fluorescence and much thicker CWs than the MCs. Carolin *et al.* (1975) mentioned different staining of the mesophyll and BS CW by electron microscopy; however, no differences were observed in the present study. Nevertheless, most of the thickened CWs in *T. indica*, including BSCs, colourless MCs, and WS tissue, have a specific undulating distribution of cellulose microfibrils which is absent in all other tissues.

With respect to the possible functions of CW ferulic acid, it has been suggested that, in certain groups of plants (in particular in Poaceae), ferulic acid in the walls of epidermal cells absorbs UV-B radiation and protects the photosynthetic apparatus (Lichtenthaler and Schweiger, 1998). Wakabayashi *et al.* (1997) showed that increased levels of ferulic acid led to decreased CW extensibility and to significantly increased mechanical strength of tissues. In some desert plants (e.g. *Tecticornia*), in which the stem is the main carbon-assimilating organ, there is little tissue to give mechanical support; thus, the presence of ferulic acid may provide strength to the CW to support the stems. It has been shown that the quantity of ferulic acid increases under water and osmotic stresses, which was suggested to facilitate adaptation to dry and saline environments (Wakabayashi *et al.*, 1997; Fan *et al.*, 2006).

For function of C_4 photosynthesis, there needs to be resistance to loss of CO_2 from sites of C_4 acid decarboxylation in BSCs, in order for it to be assimilated effectively by Rubisco, and a number of factors contribute to this to varying degrees, depending on the species and C_4 subtype (von Caemmerer and Furbank, 2003). The BS CWs may contribute to this resistance, depending on thickness and composition, and it has long been recognized that BSCs in some C_4 species have a suberized lamella, which is thought to contribute to diffusive resistance. In *T. indica*, fluorescence and histochemical analyses indicate that BSCs lack lignin and suberization, and that the higher apparent content of ferulic acid in BSCs corresponds to a thicker CW. In the two C_4 subspecies, the BS CW is 7- to 10-fold thicker than the MC CW; thus, the thicker CW may contribute to the resistance to leakage of CO_2 from BSCs. The chloroplasts in BSCs of *T. indica* are predominantly located in a centrifugal position, which would reduce diffusive resistance through the liquid phase, and increase potential for leakage from sites of decarboxylation to the exterior of the cell. However, the mitochondria in BSCs, which are the site of C_4 acid decarboxylation via NAD-ME, are positioned internal to the chloroplasts, which is favourable for refixation of CO_2 by Rubisco in the BS chloroplasts.

Photosynthetic CO_2 exchange, carbon isotope composition, and titratable acidity

The two C_4 subspecies of *T. indica* have C_4 type $\delta^{13}C$ values (subsp. *indica* –13.7‰ and subsp. *bidens* –15.2‰) and low Γ^* values (subsp. *indica* 5.2 and subsp *bidens* 4.8 μmol CO_2 mol^{-1}, Table 4) which indicates the efficiency of function of C_4, while *T. pergranulata* has C_3

type Γ^* (34.2 μmol mol^{-1}) and C_3 type $\delta^{13}C$ values (–31.4‰). The $\delta^{13}C$ values of these species are consistent with earlier results of Carolin *et al*. (1982), who obtained values of –12.2‰ to – 14.2‰. The CO_2 response curves under 2% versus 21% O_2 show that CO_2 assimilation in *T. indica* is insensitive to O_2, which is characteristic of C_4 plants. CO_2 assimilation in *T. pergranulata* is inhibited by 21% O_2 under limiting CO_2 due to photorespiration and lack of a CO_2-concentrating mechanism. The results show the C_4 *Tecticornia* would have an advantage under conditions where CO_2 is limiting. C_3 plants often have a lower light saturation of photosynthesis than C_4 plants. However, the light response curves were similar for the C_3 and C_4 *Tecticornia* species, which may be related to the thick stems requiring high light to saturate photosynthesis.

The absence of nocturnal acidification of cell sap in all three representatives of this genus indicates that they do not have the CAM type of photosynthesis.

Possible functions of unique colourless cells

In the stem tissue of C_4 *T. indica*, there is a wreath of photosynthetic tissue near the periphery. However, this is interrupted by an unusual co-occurrence of colourless MCs and BSCs within the layers of chlorenchyma, characteristic of Kranz anatomy. The area of the colourless MCs in the longitudinal plane appears to be greater than that of the colourless BSCs. The very few plastids which occur in these cells have high levels of starch, although the Kranz BSCs are the main sites of starch storage. Analysis of the enzyme composition of the colourless MCs also showed they did not have mesophyll-type specialization for C_4 photosynthesis. Colourless MCs were not observed in the C_3 species *T. pergranulata*, which raises the question as to whether this feature may have co-evolved with evolution of C_4 photosynthesis in the genus.

There has been speculation as to how windows in some succulent species may influence photosynthesis (see Egbert and Martin, 2002). One possible function of these colourless areas within Kranz anatomy is to distribute some of the incident radiation on the tissue inside the stem. As direct sunlight is received from one side of the stem, the colourless areas may increase penetration of light to the opposite side, which could increase efficiency of photosynthesis in densely growing shoots. Recently, it was noted that windows may influence photosynthesis in some plants by illuminating the chlorenchyma from two sides, inside and outside; also, in some CAM species, there is evidence that windows increase infrared radiation inside the tissue, possibly functioning to optimize leaf temperature (C Martin, personal communication).

Another function may be mechanical, contributing to stem strength, since the multicellular network of colourless MCs have much thicker CWs than the MCs. Similar structures have been observed in many xerophytic species, where the patches of green mesophyll are interrupted by colourless cells, which can occur as fibre strands (in orders Fabales and Asterales), by modified thick-walled chlorenchyma or parenchyma sheath cells, elongated perpendicular to the surface (in Restionaceae) (Bőcher and Lyshede, 1972; Fahn and Cutler, 1992), or by separate fibres or tracheids in *Arthrocnemum* and *Salicornia* (Chenopodiaceae) (SaadEddin and Doddema, 1986; Fahn and Cutler, 1992; Keshavarzi and Zare, 2006). This type of structure was thought to have a supporting function, preventing collapse of soft chlorenchyma tissue during water stress, or this compartmentation may help prevent spread of fungal infection from one patch of chlorenchyma to others.

There is also a distinctive colourless region of cells at the tips of the reduced leaves in both the C_3 *T. pergranulata* and C_4 *T. indica* subspecies. This feature may increase penetration of light into the photosynthetic cortex of the tissue. Also, in *Suaeda monoica*, two translucent gaps have been observed at the edges of leaves (Shomer-Ilan *et al*., 1975; Schütze *et al*., 2003).

Conclusions

Family Chenopodiaceace has many C_4 species occurring in three subfamilies, Chenopodioideae, Salsoloideae, and Suaedoideae. However, in species of subfamily Salicornioideae, which have stems as the major photosynthetic organ, *Tecticornia indica* s. l. and an undescribed taxon *Tecticornia* 'Yanneri Lake' form a single well-supported clade which appear to be the only C_4 lineages in the subfamily (this study; K Shepherd, personal communication; Carolin *et al*., 1982). *Tecticornia indica* has an unusual type of Kranz anatomy with a network of colourless MCs surrounding the patches of MCs within the outer layer of chlorenchyma. These colourless cells, which have thick CWs and a few chloroplasts with limited development for photosynthesis, may function to give a more optimum distribution of incident radiation in the photosynthetic tissue. *Tecticornia indica* is an NAD-ME C_4 plant having chloroplast structural features, and abundance of mitochondria in BSCs, typical of this C_4 subgroup. C_4-type $\delta^{13}C$ values, low Γ^*, and O_2 insensitivity of carbon assimilation indicate effective function of C_4 photosynthesis. The positioning of the mitochondria, which is the site of C_4 acid decarboxylation, internal to the centrifugally located BS chloroplasts, and the thickened BS CWs may support efficient donation of CO_2 to Rubisco. This study describes a unique C_4 structural type of anatomy, Kranz-tecticornoid, in the genus *Tecticornia*. Further research is needed on *Tecticornia* species and subspecies to determine if there is more diversity in forms of photosynthesis in the genus (i.e. other C_4 species, or C_3–C_4 intermediates), and to determine through structural and phylogenetic studies how C_4 may have evolved in this subfamily.

Supplementary material

The Supplementary material available at *JXB* online consists of one figure and one table. They show the phylogenetic position within *Tecticornia* of taxa analysed in this study based on ITS sequence data. Table S1 lists the taxa sequenced and Fig. S1 shows a phylogram.

Acknowledgements

This material is based upon work supported by the National Science Foundation under Grant nos IBN-0236959 and IBN-0641232, by Civilian Research and Development Foundation grants RB1-2502-ST-03 and RUB1-2829-ST-06, and by Russian Foundation of Basic Research grant 05-04-49622. HA acknowledges sabbatical and research support from the Research Council, University of Tehran (Project No. 6104037/1/01), and travel support from the Islamic Development Bank; also the help of Drs A Khan and S Gulzar during the field expedition to Pakistan. We also thank the Franceschi Microscopy and Imaging Center of Washington State University for use of their facilities and staff assistance, M Ghasemkhani and M Smith for some assistance in growing plants, C Cody for plant growth management, and Dr G Barrett for providing seeds of Australian *T. pergranulata* and *T. indica* subsp. *bidens*.

References

Akhani H, Ghasemkhani M. 2007. Diversity of photosynthetic organs in Chenopodiaceae from Golestan National Park (NE Iran) based on carbon isotope composition and anatomy of leaves and cotyledons. *Nova Hedwigia Supplementum* **131,** 265–277.

Akhani H, Barroca J, Koteeva N, Voznesenskaya E, Franceschi V, Edwards G, Ghaffari SM, Ziegler H. 2005. *Bienertia sinuspersici* (Chenopodiaceae): a new species from Southwest Asia and discovery of a third terrestrial C_4 plant without Kranz anatomy. *Systematic Botany* **30,** 290–301.

Akhani H, Edwards G, Roalson EH. 2007. Diversification of the Old World Salsoleae s.l. (Chenopodiaceae): molecular phylogenetic analysis of nuclear and chloroplast data sets and a revised classification. *International Journal of Plant Sciences* **168,** 931–956.

Akhani H, Trimborn P, Ziegler H. 1997. Photosynthetic pathways in Chenopodiaceae from Africa, Asia and Europe with their ecological, phytogeographical and taxonomical importance. *Plant Systematics and Evolution* **206,** 187–221.

Al-Turki TA, Swarupanandan K, Wilson PG. 2003. Primary vasculature in Chenopodiaceae: a re-interpretation and implications for systematics and evolution. *Botanical Journal of the Linnean Society* **143,** 337–374.

Arcihovskii VM. 1928. The growth of saxaul and the anatomical structure of its stem. *Trudy po prikladnoi botanike, genetike I selekcii* **XIX,** 287–358 [in Russian].

Bender MM, Rouhani I, Vines HM, Black CC Jr. 1973. $^{13}C/^{12}C$ ratio changes in Crassulacean acid metabolism plants. *Plant Physiology* **52,** 427–430.

Bisalputra T. 1962. Anatomical and morphological studies in the Chenopodiaceae. I. Inflorescence of *Atriplex* and *Bassia*. *Australian Journal of Botany* **10,** 13–25.

Bőcher TW, Lyshede OB. 1972. Anatomical studies in xerophytic apophyllous plants. II. Additional species from South American shrub steppes. *Biologiske Skrifter Danske Videnskabernes Selskab* **18,** 1–137.

Brooks A, Farquhar GD. 1985. Effect of temperature on the CO_2/O_2 specificity of ribulose-1,5-bisphosphate carboxylase/oxygenase and the rate of respiration in the light. *Planta* **165,** 397–406.

Carolin RC, Jacobs SWL, Vesk M. 1975. Leaf structure in Chenopodiaceae. *Botanische Jahrbücher für Systematische Pflanzengeschichte und Pflanzengeographie* **95,** 226–255.

Carolin RC, Jacobs SWL, Vesk M. 1978. Kranz cells and mesophyll in the Chenopodiales. *Australian Journal of Botany* **26,** 683–698.

Carolin RC, Jacobs SWL, Vesk M. 1982. The chlorenchyma of some members of the Salicornieae (Chenopodiaceae). *Australian Journal of Botany* **30,** 387–392.

Dengler NG, Nelson T. 1999. Leaf structure and development in C_4 plants. In: Sage RF, Monson RK, eds. C_4 *plant biology. Physiological ecology series*. San Diego: Academic Press, 133–172.

Edwards GE, Franceschi VR, Voznesenskaya EV. 2004. Single cell C_4 photosynthesis versus the dual-cell (Kranz) paradigm. *Annual Review of Plant Biology* **55,** 173–196.

Egbert KJ, Martin CE. 2002. The influence of leaf windows on the utilization and absorption of radiant energy in seven desert succulents. *Photosynthetica* **40,** 35–39.

Fahn A, Arzee T. 1959. Vascularization of articulated Chenopodiaceae and the nature of their fleshy cortex. *American Journal of Botany* **46,** 330–338.

Fahn A, Cutler DF. 1992. *Xerophytes. Encyclopedia of plant anatomy,* Vol. XIII. Part 3. Berlin: Gebruder Borntraege.

Fan L, Linker R, Gepstein S, Tanimoto E, Yamamoto R, Neumann PM. 2006. Progressive inhibition by water deficit of cell wall extensibility and growth along the elongation zone of maize roots is related to increased lignin metabolism and progressive stelar accumulation of wall phenolics. *Plant Physiology* **140,** 603–612.

Fisher DD, Schenk HJ, Thorsch JA, Ferren WR Jr. 1997. Leaf anatomy and subgeneric affiliation of C_3 and C_4 species of *Suaeda* (Chenopodiaceae) in North America. *American Journal of Botany* **84,** 1198–1210.

Freitag H, Stichler W. 2000. A remarkable new leaf type with unusual photosynthetic tissue in a central Asiatic genus of Chenopodiaceae. *Plant Biology* **2,** 154–160.

Gamaley YV. 1985. The variations of the Kranz-anatomy in Gobi and Karakum plants. *Botanicheskii Zhurnal* **70,** 1302–1314 (in Russian).

Gutierrez M, Gracen VE, Edwards GE. 1974. Biochemical and cytological relationships in C_4 plants. *Planta* **119,** 279–300.

Harris PJ, Hartley RD. 1976. Detection of bound ferulic acid in cell walls of the Graminea by ultraviolet fluorescence microscopy. *Nature* **259,** 508.

Harris PJ, Hartley RD. 1980. Phenolic constituents of the cell walls of monocotyledons. *Biochemical Systematics and Ecology* **8,** 153.

Hartley RD, Harris PJ. 1981. Phenolic constituents of the cell walls of dicotyledons. *Biochemical Systematics and Ecology* **9,** 189–203.

Hattersley PW. 1987. Variations in photosynthetic pathway. In: Soderstrom TR, Hilu KW, Campbell CS, Barkworth ME, eds. *Grass systematics and evolution*. Washington, DC: Smithsonian Institution Press, 49–64.

Jacobs SWL. 2001. Review of leaf anatomy and ultrastructure in the Chenopodiaceae (Caryophyllales). *Journal of the Torrey Botanical Society* **128,** 236–253.

Kadereit G, Mucina L, Freitag H. 2006. Phylogeny of Salicornioideae (Chenopodiaceae): diversification, biogeography, and evolutionary trends in leaf and flower morphology. *Taxon* **55,** 617–642.

Kadereit G, Borsch T, Weising K, Freitag H. 2003. Phylogeny of Amaranthaceae and Chenopodiaceae and the evolution of C_4 photosynthesis. *International Journal of Plant Sciences* **164,** 959–986.

Kapralov MV, Akhani H, Voznesenskaya E, Edwards G, Franceschi VR, Roalson EH. 2006. Phylogenetic relationships in the Salicornioideae/Suaedoideae/Salsoloideae s.l. (Chenopodiaceae) clade and a clarification of the phylogenetic position of *Bienertia* and *Alexandra* using multiple DNA sequence datasets. *Systematic Botany* **31,** 571–585.

Keshavarzi M, Zare G. 2006. Anatomical study of Salicornieae Dumort. (Chenopodiaceae Vent.) native to Iran. *International Journal of Botany* **2,** 278–285.

Ku MSB, Edwards G, Tanner CB. 1977. Effects of light, carbon dioxide, and temperature on photosynthesis, oxygen inhibition of photosynthesis, and transpiration in *Solanum tuberosum*. *Plant Physiology* **59,** 868–872.

Laisk A, Edwards GE. 1997. CO_2 and temperature-dependent induction in C_4 photosynthesis: an approach to the hierarchy of rate-limiting processes. *Australian Journal of Plant Physiology* **24,** 505–516.

Lichtenthaler HK, Schweiger J. 1998. Cell wall bound ferulic acid, the major substance of the blue-green fluorescence emission of plants. *Journal of Plant Physiology* **152,** 272–282.

Long JJ, Berry JO. 1996. Tissue-specific and light-mediated expression of the C_4 photosynthetic NAD-dependent malic enzyme of amaranth mitochondria. *Plant Physiology* **112,** 473–482.

Maurino VG, Drincovich MF, Andreo CS. 1996. NADP-malic enzyme isoforms in maize leaves. *Biochemistry and Molecular Biology International* **38,** 239–250.

Metcalfe CR, Chalk L. 1950. *Anatomy of the dicotyledons; leaves, stem, and wood in relation to taxonomy, with notes on economic uses*. Oxford: Clarendon Press.

Monteil P. 1906. Anatomie comparee de la feuille des Chenopodiacees. Thèse pour l'obtention du diplome de Docteur de l'Universite de Paris, Vol. 4, Lons-le-Saunier.

Ohsugi R, Murata T, Chonan N. 1982. C_4 syndrome of the species in the Dichotomiflora group of the genus *Panicum* (Gramineae). *Botanical Magazine Tokyo* **95,** 339–347.

Olesen P. 1974. Leaf anatomy and ultrastructure of chloroplasts in *Salsola kali* L. as related to the C_4-pathway of photosynthesis. *Botaniske Notiser* **127,** 352–363.

Pyankov VI. 1991. The origin and evolution of C_4 metabolism of the Chenopodiaceae as a result of global aridization of climate. In: Abrol YP, Wattal PN, Gnaham A, eds. *Impact of global climatic changes on photosynthesis and plant productivity*. New Delhi: Oxford & IBH, 711–720.

Pyankov VI, Artyusheva EG, Edwards GE, Soltis PS. 2001*b*. Phylogenetic analysis of tribe Salsoleae of Chenopodiaceae based on ribosomal ITS sequences: implications for the evolution of photosynthetic types. *American Journal of Botany* **88,** 1189–1198.

Pyankov VI, Voznesenskaya EV, Kondratschuk AV, Black CC Jr. 1997. A comparative anatomical and biochemical analysis in *Salsola* (Chenopodiaceae) species with and without a Kranz type leaf anatomy: a possible reversion of C_4 to C_3 photosynthesis. *American Journal of Botany* **84,** 597–606.

Pyankov VI, Voznesenskaya EV, Kuz'min AN, Ku MSB, Ganko E, Franceschi VR, Black CC Jr, Edwards GE. 2000. Occurrence of C_3 and C_4 photosynthesis in cotyledons and leaves of *Salsola* species (Chenopodiaceae). *Photosynthesis Research* **63,** 69–84.

Pyankov VI, Ziegler H, Kuz'min A, Edwards GE. 2001*a*. Origin and evolution of C_4 photosynthesis in the tribe Salsoleae (Chenopodiaceae) based on anatomical and biochemical types in leaves and cotyledons. *Plant Systematics and Evolution* **230,** 43–74.

Redondo-Gómez S, Wharmby C, Moreno FJ, De Cires A, Castillo JM, Luque T, Davy AJ, Figueroa ME. 2005. Presence of internal photosynthetic cylinder surrounding the stele in stems of the tribe Salicornieae (Chenopodiaceae) from SW Iberian Peninsula. *Photosynthetica* **43,** 157–159.

Rudall PJ, Caddick LR. 1994. Investigation of the presence of phenolic compounds in monocotyledonous cell walls, using UV fluorescence microscopy. *Annals of Botany* **74,** 483–491.

Ruzin SE. 1999. *Plant microtechnique and microscopy*. Oxford: Oxford University Press.

SaadEddin R, Doddema H. 1986. Anatomy of the 'extreme' halophyte *Arthrocnemum fruticosum* (L.) Moq. in relation to its physiology. *Annals of Botany* **57,** 531–544.

Sage RF, Li M, Monson RK. 1999. The taxonomic distribution of C_4 photosynthesis. In: Sage RF, Monson RK, eds. *C_4 plant biology*. New York: Academic Press, 551–584.

Sage RF, Monson RK. 1999. *C_4 plant biology*. San Diego: Academic Press.

Schütze P, Freitag H, Weising K. 2003. An integrated molecular and morphological study of the subfamily Suaedoideae Ulbr. (Chenopodiaceae). *Plant Systematics and Evolution* **239,** 257–286.

Shepherd KA, Macfarlane TD, Colmer TD. 2005. Morphology, anatomy and histochemistry of Salicornioideae (Chenopodiaceae) fruits and seeds. *Annals of Botany* **95,** 917–933.

Shepherd KA, Waycott M, Calladine A. 2004. Radiation of the Australian Salicornioideae (Chenopodiaceae) based on evidence from nuclear and chloroplast DNA sequences. *American Journal of Botany* **91,** 1387–1397.

Shepherd KA, Wilson PG. 2007. Incorporation of the Australian genera *Halosarcia*, *Pachycornia*, *Sclerostegia* and *Tegicornia* into *Tecticornia* (Salicornioideae, Chenopodiaceae). *Australian Systematic Botany* **20,** 319–331.

Shomer-Ilan A, Beer S, Waisel Y. 1975. *Suaeda monoica*, a C_4 plant without typical bundle sheaths. *Plant Physiology* **56,** 676–679.

Sun J, Edwards GE, Okita TW. 1999. Feedback inhibition of photosynthesis in rice measured by O_2 dependent transients. *Photosynthesis Research* **59,** 187–200.

Vasilevskaya VK. 1955. Features of structure of aphyllous xerophytes (*Haloxylon aphyllum* (Minkw.) Iljin. *Izvestija of Academy of Sciences of Turkmen SSR* **3,** 53–60 [in Russian].

Vasilevskaya VK, Butnik AA. 1981. The types of the anatomical structure of the dicotyledon leaves (a contribution to the method of anatomical description). *Botanicheskii Zhurnal* **66,** 992–1001 [in Russian].

von Caemmerer S, Farquhar GD. 1981. Some relationships between the biochemistry of photosynthesis and the gas exchange of leaves. *Planta* **153,** 376–387.

von Caemmerer S, Furbank RT. 2003. The C_4 pathway: an efficient CO_2 pump. *Photosynthesis Research* **77,** 191–207.

Vosnesenskaya EV, Steshenko AP. 1974. Morphological and anatomical characteristics of shoots of saxaul. *Botanicheskii Zhurnal* **59,** 102–110 [in Russian].

Voznesenskaya EV. 1976*a*. The ultrastructure of assimilating organs of some species of the family Chenopodiaceae. II. *Botanicheskii Zhurnal* **61,** 1546–1557 [in Russian].

Voznesenskaya EV. 1976*b*. The ultrastructure of assimilating organs in some species of Chenopodiaceae family. I. *Botanicheskii Zhurnal* **61,** 342–251 [in Russian].

Voznesenskaya EV, Artyusheva EG, Franceschi VR, Pyankov VI, Kiirats O, Ku MSB, Edwards GE. 2001. *Salsola arbusculiformis*, a C_3–C_4 intermediate in Salsoleae (Chenopodiaceae). *Annals of Botany* **88,** 337–348.

Voznesenskaya EV, Chuong S, Koteyeva N, Franceschi VR, Freitag H, Edwards GE. 2007. Structural, biochemical and physiological characterization of C_4 photosynthesis in species having two vastly different types of Kranz anatomy in genus *Suaeda* (Chenopodiaceae). *Plant Biology* **9,** 745–757.

Voznesenskaya EV, Franceschi VR, Artyusheva EG, Black CC Jr, Pyankov VI, Edwards GE. 2003. Development of the C_4 photosynthetic apparatus in cotyledons and leaves of *Salsola richteri* (Chenopodiaceae). *International Journal of Plant Sciences* **164,** 471–487.

Voznesenskaya EV, Franceschi VR, Kiirats O, Artyusheva EG, Freitag H, Edwards GE. 2002. Proof of C_4 photosynthesis without Kranz anatomy in *Bienertia cycloptera* (Chenopodiaceae). *The Plant Journal* **31,** 649–662.

Voznesenskaya EV, Gamaley YV. 1986. The ultrastructural characteristics of leaf types with Kranz-anatomy. *Botanicheskii Zhurnal* **71,** 1291–1307 [in Russian].

Wakabayashi K, Hoson T, Kamisaka S. 1997. Osmotic stress suppresses cell wall stiffening and increase in cell wall-bound ferulic and diferulic acids in wheat coleoptiles. *Plant Physiology* **113,** 967–973.

Walker RP, Acheson RM, Tecsi LI, Leegood RC. 1997. Phosphoenolpyruvate carboxykinase in C_4 plants: its role and regulation. *Australian Journal of Plant Physiology* **24,** 459–468.

Werker E, Fahn A. 1966. Vegetative shoot apex and the development of leaves in articulated Chenopodiaceae. *Phytomorphology* **16,** 393–401.

Wilson PG. 1980. A revision of the Australian species of Salicornieae (Chenopodiaceae). *Nuytsia* **3,** 100–154.

Wingler A, Walker RP, Chen ZH, Leegood RC. 1999. Phosphoenolpyruvate carboxykinase is involved in the decarboxylation of aspartate in the bundle sheath of maize. *Plant Physiology* **120,** 539–545.